Urban Climate 46 (2022) 101288

Contents lists available at ScienceDirect

Urban Climate

journal homepage: www.elsevier.com/locate/uclim

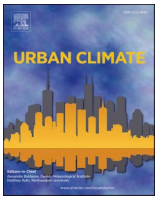

How do street trees affect urban temperatures and radiation exchange? Observations and numerical evaluation in a highly compact city

Ricard Segura [a], E. Scott Krayenhoff [b], Alberto Martilli [c], Alba Badia [a], Carme Estruch [a], Sergi Ventura [a], Gara Villalba [a,d,*]

[a] Sostenipra Research Group (SGR 01412), Institute of Environmental Sciences and Technology (MDM-2015-0552), Universitat Autònoma de Barcelona (UAB), Z Building, Campus UAB, 08193 Bellaterra, Barcelona, Spain
[b] School of Environmental Sciences, University of Guelph, Guelph, ON N1G 2W1, Canada
[c] Research Center for Energy, Environment and Technology, CIEMAT, Madrid, Spain
[d] Department of Chemical, Biological and Environmental Engineering, Universitat Autònoma de Barcelona (UAB), Campus UAB, 08193 Bellaterra, Barcelona, Spain

ARTICLE INFO

Keywords:
Street trees
Urban vegetation
Thermal regulation
Urban canopy model

ABSTRACT

Street trees are an important driver of street microclimate through shading and transpirative cooling, which are key mechanisms for improving thermal comfort in urban areas. Urban canopy models (UCM) with integrated trees are useful tools because they represent the impacts of street trees on neighborhood-scale climate, resolving the interactions between buildings, trees and the atmosphere. In this study, we present the results of a measurement campaign where vehicle transects were completed along two similar parallel streets of Barcelona with different tree densities, recording upward and downward radiation fluxes, air temperature and humidity at street level. These observations are used to evaluate and improve the multi-layer UCM Building Effect Parameterization with Trees (BEP-Tree). Prior simulations of the model revealed insufficient heat exchange between the canyon surfaces and the air at the lowest vertical levels inside the deep canyons, which we solve by including turbulent buoyancy driven wind velocity in the model. Air temperatures are on average 1.3 °C higher in the street with sparser trees when wind direction is perpendicular to the streets. The BEP-Tree simulations demonstrate good agreement with the observations in terms of temperature and radiation, and capture the diurnal evolution of temperature and radiation between the two streets.

1. Introduction

Climatic conditions in urban areas are likely to worsen in the near future if unaddressed, due to risks deriving from climate change, such as heat extreme events (Revi et al., 2014), and the added climatic stresses present in urban areas (Oke, 1982, Oke et al., 2017; Arnfield, 2003). The increasing urbanization and densification of cities is also an added challenge that urban planners and local governments must manage in order to preserve the city's environmental sustainability. The implementation of urban green

* Corresponding author at: Sostenipra Research Group (SGR 01412), Institute of Environmental Sciences and Technology (MDM-2015-0552), Universitat Autònoma de Barcelona (UAB), Z Building, Campus UAB, 08193 Bellaterra, Barcelona, Spain.
E-mail address: gara.villalba@uab.cat (G. Villalba).

https://doi.org/10.1016/j.uclim.2022.101288
Received 5 May 2022; Received in revised form 5 August 2022; Accepted 12 September 2022
Available online 25 September 2022

infrastructure in urban planning strategies can help adapt cities to changing climates, improve public health, promote social cohesion, and provide with other beneficial services (Demuzere et al., 2014; Baró et al., 2019).

The moderating effect of urban vegetation on urban temperatures has been well assessed in the literature (Bowler et al., 2010; Oliveira et al., 2011; Zhang et al., 2013; Krayenhoff et al., 2021), evidencing the associated reductions of air and surface temperatures at different scales in the city (Oke, 1989; Shiflett et al., 2017). At local and neighborhood scale, large vegetated patches modify the surface energy balance through the evapotranspiration process, cooling the air around the vegetation and providing a thermal reduction of the surrounding urban areas (Grimmond and Oke, 1991; Grimmond et al., 1996). At microscale, trees provide shade to the surrounding built surfaces and to the pedestrians, modifying the biometeorological conditions experienced by them and improving thermal comfort (Coutts et al., 2016; Middel and Krayenhoff, 2019).

In particular, street trees are a key factor in the evolution of the local climate inside the street canyon, altering the radiation, momentum and convective heat exchange between the buildings and the atmosphere (Oke, 1989; Krayenhoff et al., 2020). Street trees can play an important role in the greening of high-compact cities (limited horizontal extension but high building density), due to the low capability of these cities to integrate large urban green infrastructure measures (Baró et al., 2019). The extent to which street trees can improve air temperatures and increase the resilience of these areas to heat events depends on different aspects that influence the magnitude of cooling, such as the canyon geometry and sun-orientation, the local meteorological conditions, the geographic setting of the city, the amount of tree canopy covering the canyon floor and distribution, tree typology, the water availability for trees and the tree health condition (Gillner et al., 2015; Coutts et al., 2016; Salmond et al., 2016; Krayenhoff et al., 2020).

Although numerous observational and numerical studies have focused on investigating the cooling effects of trees in urban parks (Shashua-Bar and Hoffman, 2000; Bowler et al., 2010; Lin and Lin, 2010; Oliveira et al., 2011; Papangelis et al., 2012), less research has been centered over the neighborhood-scale cooling impact of street trees (Krayenhoff et al., 2020). Johansson and Emmanuel (2006) found that the most comfortable air conditions were found in deep canyons, especially if tree shade is present, compared to open and wide streets, for a humid and hot city in southeast Asia. Coutts et al. (2016) observed daytime air temperature reductions of 0.2 to 0.6 °C in a shallow street with dense tree canopy compared to another street with more sparse tree presence in Melbourne, Australia. They also observed that the cooling impact of trees was lower in a deep canyon with similar tree density because the shading effect of trees was exceeded by the shading effect of the tall buildings. Moreover, street trees may increase nocturnal air temperatures under the canopies, due to the reduced sky view factor (SVF), which inhibits the cooling of canyon surfaces due to longwave radiation release (Bowler et al., 2010). This effect can exacerbate possible health issues during heat events due to the uncomfortable temperatures at night (Salmond et al., 2016).

Due to the increased necessity of assessing the impacts of street trees in pedestrian level climate and to avoid the dependence on costly observation campaigns, the effect of street trees on local climate has been recently included in diverse neighborhood-scale urban canopy models (Lee and Park, 2008; Lee, 2011; Ryu et al., 2016; Krayenhoff et al., 2020; Meili et al., 2020). These models are able to represent the radiation exchange, energy balance, hydrodynamic or hydrological processes related with street trees, or a combination of these processes. These models can be alternatively coupled with regional climate models to assess the cooling potential of street trees at city scale and to further improve the capabilities of these models for urban climate applications (Mussetti et al., 2020). The Building Effect Parameterization with Trees (BEP-Tree; Krayenhoff et al., 2020) is a multi-layer urban canopy model (UCM) that accounts for the integrated effects of streets trees on the neighborhood-scale climate, in terms of radiation exchange, energy balance, wind drag, turbulence and pedestrian level climate. The model has been thoroughly evaluated in Krayenhoff et al. (2020), via comparison against measurement datasets of different treed urban neighborhoods in three cities (Vancouver and London in Canada, and Salt Lake City in USA), spanning from microscale to neighborhood scale. However, these three sets of measurements correspond to open lowrise residential neighborhoods, characterized by a low density of impervious area and a low building height to street width ratio (H/W). Therefore, model evaluation is still lacking for more compact areas with H/W greater than one, and bigger building-to-plan area fractions (λ_p), where the impacts of street trees on pedestrian climate can affect a higher population density.

In this context, there is much interest in the assessment of the effects of street trees on local climates in highly compact cities, where the high density of urban dwellers and intense traffic activities require urban planners to focus on urban design for improved thermal regulation. The main objectives of this research are:

1. Evaluate and improve the ability of a neighborhood-scale urban canopy model that integrates the effect of trees inside the canyon (i.e. BEP-Tree) to reproduce the local and microclimatic conditions inside the street canyons in a highly-compact city.
2. Combine data from an observational campaign and numerical results to assess the microscale air cooling and radiation exchange effects of street trees inside highly-compact cities.

To achieve these objectives, we perform a micrometeorological measurement campaign in the city of Barcelona (Spain) for two cloud-free summer days. Vehicle transects were completed along two parallel streets with different tree densities but similar street geometry, recording upward and downward radiation fluxes, air temperature and humidity. These data are used to evaluate the ability of the BEP-Tree model to reproduce the micrometeorology of this scenario. Finally, the meteorological simulations and the experimental data are used to evaluate the combined impacts of vegetation and buildings on urban canopy layer climate.

2. Methodology

2.1. BEP-tree model

2.1.1. The standard BEP-tree model description

The BEP-Tree model integrates the effects of street trees in the urban canopy layer within the Building Effect Parameterization (BEP) (Martilli et al., 2002). The BEP model is a multi-layer urban canopy scheme that accounts for the impact of buildings on airflow and computes the surface energy exchange between urban vertical and horizontal surfaces (building walls and roofs and street ground) and the atmosphere. This scheme derives neighborhood-scale averaged fluxes and local climate conditions at different vertical levels within the canopy to serve as surface boundary conditions in mesoscale atmospheric models. BEP parameterizes the impact of a regular arrangements of buildings on wind, turbulent kinetic energy, potential temperature, and specific humidity. The scheme computes the effect of urban geometry on the longwave (thermal radiation) and shortwave (solar radiation) radiation fluxes, considering the effect of reflections, shadowing and radiation trapping to derive the urban surface temperature evolution.

In the BEP-Tree model, BEP model is modified to include a one-dimensional vertical turbulent diffusion model (Santiago and Martilli, 2010), as well as an entirely new radiation scheme (Krayenhoff et al., 2014). This modification allows it to perform offline 1-D simulations uncoupled from a mesoscale atmospheric model. It only requires an atmospheric forcing at the top boundary of a vertical column, usually two-three times the mean building height. Street trees are not explicitly resolved, but the interaction with the incoming and outgoing radiation inside the canyons is parameterized based on a leaf area vertical density profile and a street canyon-average foliage clumping factor. The multi-layer approach of the model allows the representation of vertical distribution of building heights probabilities and leaf area density profiles, representing trees between and above buildings.

The built and leaf surface energy balances are derived in order to generate sink and sources of temperature and humidity to the vertical diffusion equations in the one-dimensional model. The multi-layer radiation model of BEP-Tree uses ray-tracing to determine the direct shortwave exposure of all urban canyon elements at each time step (Krayenhoff et al., 2014). Furthermore, view factors between all built and foliage elements are computed once at the start of the simulation using a Monte-Carlo ray tracing approach and then the model solves all longwave and diffuse shortwave exchange at each model timestep using a radiosity approach. Vegetation intercepts shortwave and longwave radiation according to the Beer-Lambert-Bouguer law:

$$\Delta V_i(iz) = r_i[1 - exp(-K_{bs}\Omega L_D(iz)\Delta sf_i)] \quad (1)$$

where $\Delta V_i(iz)$ is the reduction of ray intensity due to the tree foliage at vertical layer iz (W m^{-2}), r_i is the initial intensity of the ray (W m^{-2}), K_{bs} is the foliage extinction coefficient, Ω is a foliage clumping factor, $L_D(iz)$ is the leaf area density at vertical level iz, Δs is the 2-D ray step size (m) and f_i is the ratio of 3-D (actual) to 2-D (model) distance travelled by the ray (depends on the canyon orientation to the sun) (Krayenhoff et al., 2014). The clumping factor is used to model the heterogeneous distribution of tree crowns in the canyon. The clumping factor ranges between 0 and 1, being 1 when foliage is randomly distributed within the canyon. For canyon spaces and tree crown scale clumping it is approximated as follows:

$$\Omega = \frac{-1}{0.5LAI_{can}} ln\left(1 - \lambda_{v,can}(1 - exp(-0.5LAI_{tree}))\right) \quad (2)$$

where LAI_{can} and LAI_{tree} are street-canyon average and tree crown space-average leaf area indices, and $\lambda_{v,\,can}$ is the fraction of plan area coverage of tree crowns inside the street canyon (Krayenhoff et al., 2020).

BEP-Tree also includes a parameterization of building and tree effects on airflow inside the urban canopy layer (Martilli et al., 2002; Santiago and Martilli, 2010; Krayenhoff et al., 2015, 2020). BEP-Tree considers the sink effect for momentum of both building and foliage elements, due to the inclusion of form drag in the horizontal momentum conservation equation proposed in Santiago and Martilli (2010). Correspondingly, BEP-Tree also includes terms of enhanced turbulent kinetic energy due to wake production generated by the buildings and foliage drag. Moreover, turbulent length scales were updated based on the comparison of Large-Eddy Simulations (LES) and wind tunnel measurements (Nazarian et al., 2020) to account for building effects on the flow.

The required inputs of the model are meteorological forcing at the top level (within the inertial sublayer, roughly 2–3 times the mean building height) and geometric, radiative and thermal variables of the canyon including the vegetation. The forcing can be provided from an observation tower placed over the maximum roughness element in the urban area or from a mesoscale model. The geometric variables of the canyon are building height distribution and width, street width, thermal and radiative parameters of the building materials, the leaf area density vertical profile and the clumping factor. Further details about the model equations and parameterizations can be found in Krayenhoff et al. (2014, 2015, 2020).

2.1.2. A new buoyancy driven wind velocity parameterization

Our preliminary simulations using the BEP-Tree model for this highly-compact case indicated that the model had some limitations in terms of representing wind speed inside deep, narrow canyons during the central hours of the day with strong surface heating. These initial BEP-Tree simulations had small sensible heat transfer from building walls and street to the canopy air that we interpret as caused by an underestimation of wind speed in the lower levels of the street canyon. Moreover, reduced turbulent mixing inside the canyon and anomalously high surface and air temperatures in the lower levels of the canyon were also found (see Section 4.1). This may be caused by the modified drag coefficients and turbulent length scales in the model, which were updated based on LES simulations (Nazarian et al., 2020). Nazarian et al. (2020) investigated the turbulent flow around idealized urban configurations with aligned and

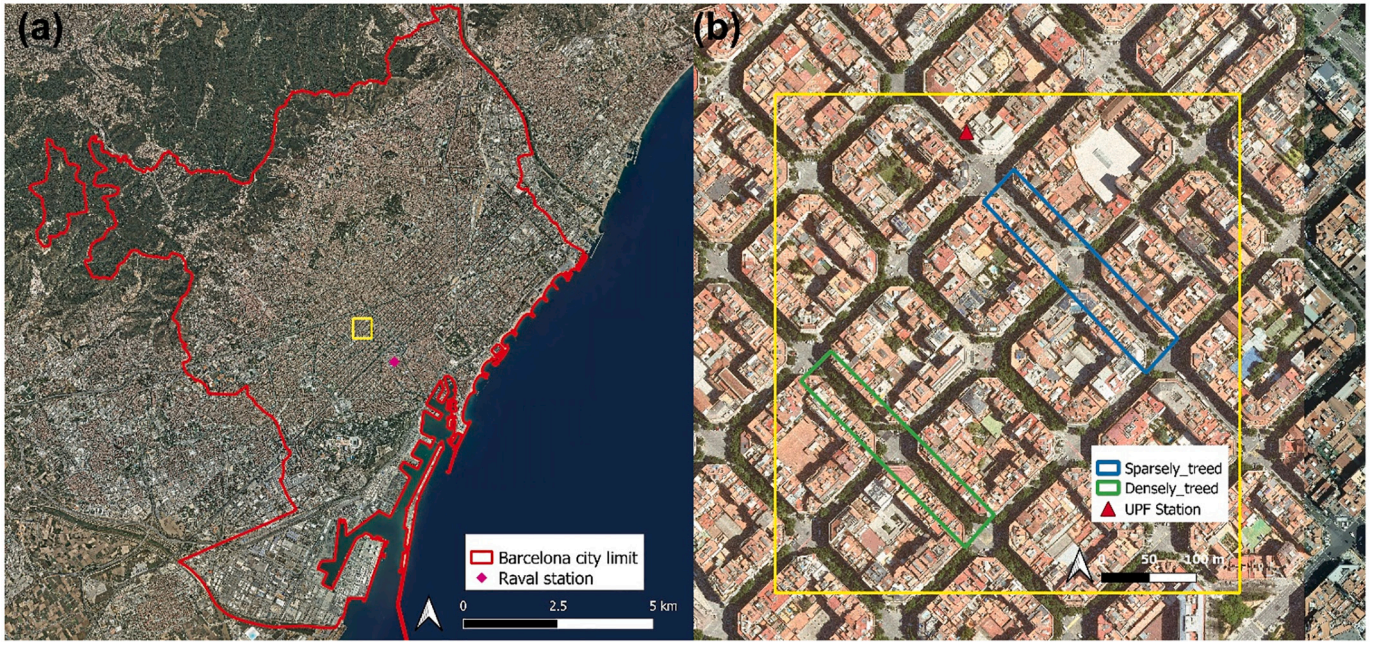

Fig. 1. (a) Administrative boundaries of Barcelona city; (b) detail of the region of study in the Eixample neighborhood with the two studied streets: Sparsely_treed (blue) and Densely_treed (green). The Raval station is marked with a pink diamond and the UPF station is marked with a red triangle. (For interpretation of the references to colour in this figure legend, the reader is referred to the web version of this article.)

staggered cube arrays with different packing densities (λ_p = 0.0625–0.44) and height-to-width ratios (H/W < 1.0). The studied geometrical conditions with the LES simulations do not fully cover the geometric conditions of highly-compact cities, with packing densities over 0.5 and height-to-width ratios exceeding 1. Moreover, LES simulations were performed under neutral conditions, which clearly differ from the unstable canyon conditions observed during hot summer days in temperate cities, with a high amount of solar radiation absorbed by the urban surfaces. Additionally, Nazarian et al. (2020) also concluded that spatially averaged kinetic energy was still underestimated in the lowest levels closest to the ground in highly compact configurations in UCM simulations with the updated length scales.

For this reason, we have hypothesized that vertical air movements in the canyon are largely caused by buoyancy effects with characteristic length scales equal to the depth of the deep urban canopy which are not captured by the local formulation of the dynamics in the model. Therefore, a buoyancy driven turbulent wind velocity is defined to increase the aerodynamic conductance within the urban canyon, similar to the free convection velocity (w^*) term proposed by Lemonsu et al. (2004) to represent the urban canopy layer in the dense city of Marseille, France. This buoyancy driven wind velocity has been derived with dimensional analysis using the building height z_m, the buoyancy parameter g/θ_0, where g is the gravity acceleration and θ_0 corresponds to a reference potential temperature which has been defined to 300 K, and the difference in potential temperature between the lowest model level, θ_1 (0.5 m), and θ_m the potential temperature at the building height level, as follows:

$$w^* = \sqrt{\frac{z_m{}^* g^* (\theta_1 - \theta_m)}{\theta_0}} \tag{3}$$

This equation is used for unstable conditions ($\theta_1 > \theta_m$), while for neutral or stable conditions the non-local production of buoyancy generated turbulence is expected to be zero ($w^* = 0$). A sensitivity analysis of the impact of this new parameterization is shown in section 3.1.

2.2. Study area

2.2.1. The city of Barcelona

The city of Barcelona is situated in the northeast coast of the Iberian Peninsula, in the western Euro-Mediterranean region. The city coastline is oriented from southwest to northeast, and the city is bounded at the northwest by the mountainous region of the Collserola Natural Park (almost 500 m of altitude), and at the northeast and southwest by two rivers (Fig. 1a). The city covers an extension of 101.4 km^2 from which 17.0 km^2 belongs to the Collserola Natural Park and 11.7 km^2 are urban green areas (Barcelona City Council Statistical Yearbook, 2021). Barcelona has a population of 1.66 million inhabitants, with an average density of 163 inhabitants/ha and maximum values over 400 inhabitants/ha in some neighborhoods in the city center. The city of Barcelona is characterized principally by two urban geometries: the first one is represented by the Eixample district (7.5 km^2) with regular block patterns, wide avenues and two street orientations (perpendicular and parallel to the coast); and the second one represented by the old neighborhoods of Gràcia, Raval and Gòtic (1.3 km^2, 1.1 km^2 and 0.8 km^2) with narrow streets and unregular patterns. The Eixample district is the most populated (269,341 inhabitants in 2021) and densest district in the city of Barcelona with 361 inhabitants/ha; and has the lowest coverage of urban greenness per inhabitant with 2.0 m^2/inhabitant.

Despite the high compactness and density of the city and the low number of green urban areas per inhabitant (7.0 m^2/inhabitant on average in the entire city), Barcelona has a large number of street trees (157,636 trees), with 95 trees per 1000 inhabitants, which is well above the average range of other European cities (50–80 trees per 1000 inhabitants) (Pauleit et al., 2002; Baró et al., 2019). Moreover, the municipal government has a complete inventory of all the street trees and palm trees updated every 4 months, including information such as geographic coordinates, species name and other structural and health condition variables (available in https://opendata-ajuntament.barcelona.cat/data/ca/dataset/arbrat-viari).

2.2.2. The experiment site

Two parallel streets inside the District of the Eixample are studied due to the high compactness of the buildings and the regularity of the block pattern (Fig. 1b). The regular form of the urban canopy in the two horizontal directions facilitates that the observed values resemble the neighborhood-scale average for street of this orientation. The two streets are oriented perpendicular to the coast (from NW to SE) and have different tree covers and tree species: the Balmes street (Sparsely_treed) exhibits a sparse and short tree cover with a low tree canopy fraction in the urban canyon (16% tree canopy cover within the urban canyon area), while the Aribau street (Densely_treed) exhibits a dense and tall tree cover (65% tree canopy fraction in the urban canyon). The street trees in Sparsely_treed are composed of *Tilia x euchlora* which have a mean height of 5.8 m and the shade only partially covers the sidewalks. On the contrary, the trees in Densely_treed are composed of *Celtis australis* and *Platanus x hispanica* which have a mean height of 10.8 m, and the shade completely covers the full width of the urban canyon.

The streets are separated by a distance of 270 m. The street width of the two canyons is obtained from Google Earth and airborne photos. The width of both streets is 20 m, with the middle 10 m of the street section composed of 4 traffic lanes and 5 m at each side devoted for pedestrian sidewalks. There is considerable traffic on both streets during daytime, especially at peak hours in the morning and afternoon. Average building heights are gathered from LiDAR data and a digital surface model with 2 m resolution, available at the Institute Cartographic and Geological of Catalonia (ICGC, 2019). Average building heights are 30.6 m and 29.0 m, for Sparsely_treed and Densely_treed streets, respectively. This yields a height-to-width ratio of 1.53 and 1.45. The building plan to area fraction (λ_p) is similar for the streets with a value of 0.82.

2.3. Observed data

Vehicle transects around the two parallel streets were performed during two consecutive summer days, 28–29 July 2021. The vehicle was equipped with a net radiometer Hukseflux NR01 suspended at 1.5 m height over the back of the car, composed of two pyrgeometers measuring longwave radiation fluxes, and two pyranometers measuring shortwave radiation fluxes, in both the upwelling and downwelling vertical directions. Moreover, the vehicle was equipped with a Kestrel 4500 pocket weather tracker that recorded meteorological variables such as air temperature, relative humidity, and pressure, as well as a GPS device to track the coordinates of the sample points. A picture of the measurement set up can be seen in Fig. S1 in the Supplementary material. The measurements from the net radiometer were recorded with a data logger Campbell Scientific CR1000 every 10 s. The meteorological measurements were also recorded at each 10 s but independently by the Kestrel device. The transects started at each exact hour o'clock and consisted of two laps around the two streets stopping between 13 and 24 times in each one of the two outermost traffic lanes, leaving the two middle traffic lanes free so that the traffic would not be disturbed. Each measurement stop lasted between 25 and 30 s to fulfil the response time of the radiometers (18 s for the 95% confidence interval). In total, each transect around the two streets took between 30 and 40 min to be completed, depending on the traffic. All the data of the different stops in each track and street is averaged and is assigned to the average time of all the stops in the same track and street. The hourly transects started at the 04 UTC (06 local time, local time is obtained adding two hours) of the 28 July 2021 until the 23 UTC of the same day, and from the 3 UTC of the 29 July 2021 to the 23 UTC of the same day. The radiometer measurements on the 29 July at the 12 UTC were not recorded due to a mechanical problem. The measurements span from before dawn until past midnight in order to study the different stability regimes of the urban canopy layer and the cooling process of the surfaces and atmosphere during the evening. The high presence of traffic until even midnight (22 UTC), generates an additional contribution of anthropogenic heating that can be expected to generate some discrepancy between the modelled and observed air temperatures (since it is not included in BEP-Tree) and affects the urban canopy layer stability.

To complete the characterization of the two streets, upper hemisphere fisheye photos were taken at 1.1 m height and randomly distributed along the street axis but at the same traffic lanes of the vehicle transects to derive the sky view factor (SVF), the vegetation view factor (VVF) and the building view factor (BVF) perceived by the up-facing radiometer. A total of 12 photos for each street (between the two outermost traffic lanes) were taken using a Canon EOS 5D Mark III and a Canon EF 8-15 mm f/4 L Fisheye USM lens. The photos were manually segmented using a photo editor program and then, the view factors were obtained using the software RayMan 1.2 (Matzarakis et al., 2010). An example of the photographs manual segmentation can be seen in Fig. S2 of the Supplementary material. The mean values of the measured view factors and the ones estimated by the BEP-Tree model can be seen in Table 1. As we can see from the table, the view factors calculation of the BEP-Tree model using the Monte-Carlo ray tracing approach can reproduce the actual values observed with the photos for the Sparsely_treed street, while it overestimates the SVF for Densely_treed, in detriment of the BVF. However, BEP-Tree view factors are for the street average, while the observed view factors are taken from the outer vehicle lane only (i.e., not a representative sample across the width of the street), so a small discrepancy is expected.

2.4. Model evaluation

2.4.1. BEP-tree urban surface parameters

Two simulations spanning from the 28 July 2021 at 00 UTC to the 30 July 2021 at 00 UTC were conducted with BEP-Tree to model the two street canyons. The vertical resolution in the model is 1 m, the maximum vertical level with buildings is 35 m for the Sparsely_treed simulation and 30 m for the Densely_treed station, and the model's upper boundary is at 70 m, approximately two times the height of the highest building, which correspond just above the top of the roughness sublayer, within the inertial sublayer (Oke et al., 2017). While inside the roughness sublayer the flow is modified by the protruding elements below, varying in the horizontal and vertical directions, in the above layer, the inertial sublayer, the flow responds to the integral effect of the urban neighborhood below. In our case, the urban morphological properties are homogenous in the horizontal, so the inertial sublayer can be considered homogenous horizontally and only vary vertically.

The model has been configured to represent just one street direction (135^{o}) to better represent the conditions inside the two urban canyons. The urban surface thermal properties have been defined based on the most common construction materials of the study area. The street is composed of asphalt and concrete, while the building walls are primarily brick and roofs are clay tiles. The material properties have been defined based on typical values of reference tables (Oke et al., 2017). The rest of the properties have been defined based on the urban parameters of local climate zone 2 in Ribeiro et al. (2021). The leaf area per tree canopy is assessed from the measured canopy height and crown width, computed from the LiDAR data and airborne photos of the canyon, respectively, and the parameterization of Nowak (1996). The street-canyon average leaf area can be approximated to be $LAI_{tree} * \lambda_{v,\ can}$. The leaf density

Table 1
Mean view factors measured from upper-hemisphere fisheye photos and computed by the BEP-Tree model for the two streets. The values in parentheses correspond to the standard deviation. SVF, VVF and BVF stand for sky view factor, vegetation view factor and building view factor.

Street	Measured			BEP-Tree		
	SVF	VVF	BVF	SVF	VVF	BVF
Sparsely_treed	0.26 (0.03)	0.19 (0.08)	0.55 (0.07)	0.248	0.139	0.613
Densely_treed	0.05 (0.03)	0.47 (0.05)	0.48 (0.03)	0.117	0.508	0.374

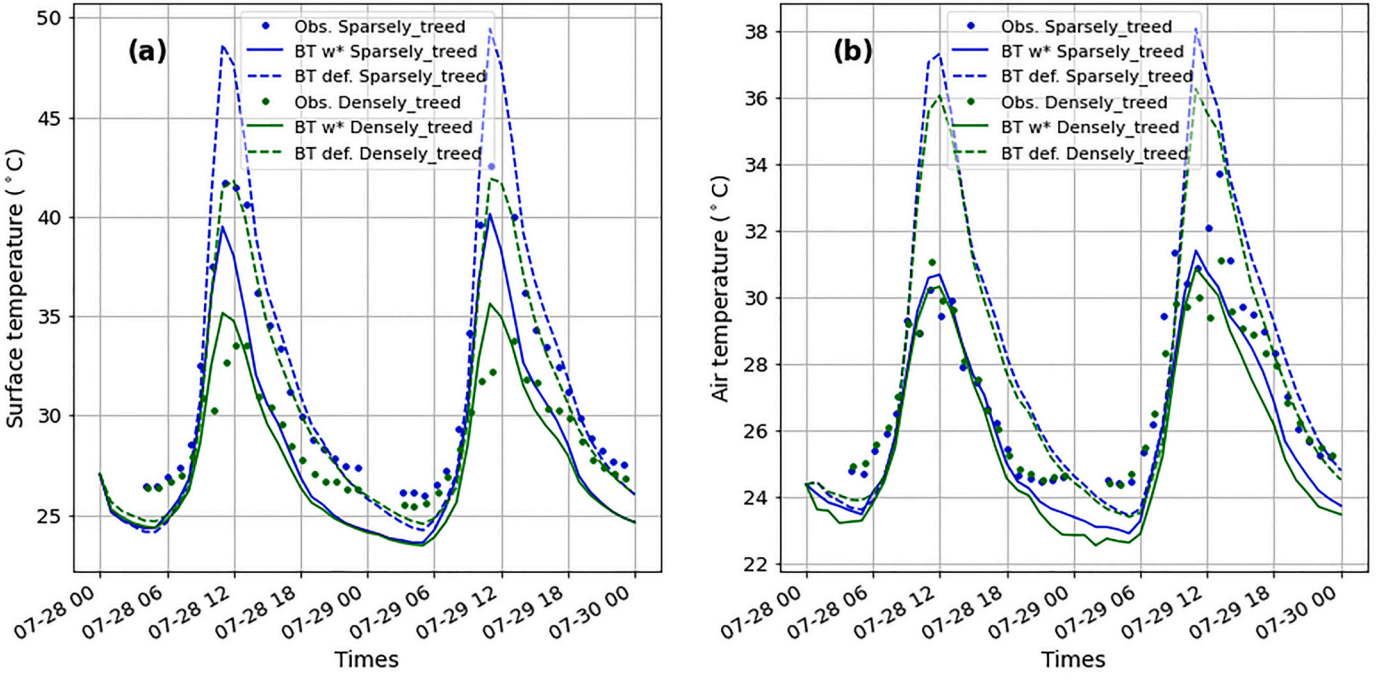

Fig. 2. Modelled with the default BEP-Tree model (BT def., dashed lines), the BEP-Tree with the buoyancy driven wind speed (BT w*, straight lines) and observed (Obs., circles) canyon averaged road surface temperature (a) and air temperature (at 1.5 m height from the ground) (b) for Sparsely_treed (blue) and Densely_treed (green) streets in Barcelona. (For interpretation of the references to colour in this figure legend, the reader is referred to the web version of this article.)

profile is derived based on the vertical distribution of total leaf area from Lalic and Mihailovic (2004). The urban canopy parameters and vegetation parameters used in the model for the two streets simulations can be seen in Table A1 of the Supplementary material.

2.4.2. Meteorological forcing

The meteorological forcing of the model at its top boundary is obtained partially from fixed meteorological station observations placed over a building rooftop of the Universitat Pompeu Fabra (UPF, see Fig. 1b) in the Sparsely_treed street. This station (at 1.5 m over the rooftop, 26.5 m over the street ground level) records downwelling shortwave and longwave radiation fluxes, and other meteorological data (air temperature, pressure, humidity). Due to the low height of the building with the station compared to the tallest buildings in the surrounding area, and the low mast height, only the radiometer measurements, specific humidity, and pressure (with a height correction to the forcing height) are used for the forcing. The rest of the meteorological variables, wind components and potential temperature are obtained from a meteorological station from the Meteorological Service of Catalonia, in the Raval neighborhood (see Fig. 1a), at 2.0 km from the study area. This station, placed over a building rooftop at 21 m over the street ground level, records 10 m (above roof top) wind speed and direction and 2 m (above roof top) air temperature. Wind speed was corrected to represent the roughness values of the study area neighborhood using the approach of Wieringa (1986), and then the components were rotated to the same directions as the street orientation (45° and 135°). The Wieringa approach consists of applying a logarithmic height profile to the observed wind speed (U_s) to obtain the mesowind (the wind at the top of the roughness sublayer, U_{70}) based on this equation:

$$U_{70} = U_s \frac{ln\left(\frac{70-z_d}{z_0}\right)}{ln\left(\frac{z_s-z_d}{z_0}\right)} \tag{4}$$

where z_s is the observation height above street level, z_d is the zero-plane displacement height at the measuring point (2/3 * z_m, where z_m is the mean building height), and z_0 is the roughness length at the measuring point (0.1 *z_m) (Grimmond and Oke, 1999).

In the case of potential temperature at the forcing height, the potential temperature measured by the Raval Station is corrected to 70 m applying a correction based on the height. According to previous mesoscale atmospheric simulations conducted with the Weather Research and Forecasting model (WRF) for the study area (Segura et al., 2021), we have determined a coefficient of reduction between the measuring height and the forcing height. This variation is mainly affecting the daytime potential temperature since the nighttime vertical profiles are close to neutral. Then, the potential temperature is corrected based on this approximation:

$$\theta_{70}(ih) = \theta_0 + \alpha_k(ih)*(\theta_s(ih) - \theta_0) \tag{5}$$

where $\theta_{70}(ih)$ is the estimated potential temperature at 70 m and time of the day ih, θ_s is the measured potential temperature at time of the day ih, θ_0 is a reference potential temperature defining the lowest value at night (295.5 K), and α_k is the adjustment parameter that depends on the time of the day. The adjustment parameter has been obtained averaging between different days the reduction potential observed in WRF simulations for the grid cell that contains the Raval station, being 0.8 during daytime (6–19 UTC) and 1.0 during nighttime (20 UTC – 5 UTC). This methodology can introduce uncertainty in the BEP-Tree model to derive the air temperature inside the urban canyon, which is discussed in Section 4 of the Supplementary material.

3. Results

3.1. Sensitivity analysis to the wind parameterization

To determine the effects produced by the buoyancy-driven wind velocity described in the Section 2.1.2 a sensitivity analysis is performed to compare the temporal evolution of air and surface temperature, along to the vertical profiles of potential temperature inside the canyon. In the case of the default BEP-Tree model, the mean wind speed of a vertical layer inside the canyon, based on the mean horizontal components ($ws(iz) = \sqrt{u^2 + v^2}$), is used to derive the aerodynamic heat conductance between the building, ground or leaf surfaces and the air, as explained in Krayenhoff et al. (2020). In the case of the new parameterization, the wind speed used for computing the aerodynamic conductance at each time step is the maximum value between ws and w^* (see Eq. (3)), which represents the buoyancy effect on turbulent vertical wind velocity. In this sensitivity analysis, we compare the BEP-Tree simulations using the default air exchange parameterization (BEP-Tree def.) and the simulations with the new thermal turbulent wind speed (BEP-Tree w^*).

When the vertical thermally driven turbulent wind speed is not considered in the model (BEP-Tree def.), a considerable increase of the road surface temperature is seen in the simulations (Fig. 2a), reaching maximum daytime road temperatures up to 9.6 °C and 7.0 °C higher than the simulations with the new parameterization for Sparsely_treed and Densely_treed streets, respectively. The low mean wind speed considered by the default BEP-Tree model in the lowest levels of the urban canyon (below 0.1 m/s) produces a low turbulent sensible heat flux between the surface and the first air level (see Fig. S4 in the Supplementary material), increasing the surface temperature. In this case, the model simulates a higher temperature range between the daytime and nighttime surface temperatures, overestimating the maximum surface temperatures (up to 7.0 °C for Sparsely_treed and up to 9.7 °C for Densely_treed) and underestimating the minimum nighttime temperatures, for the two streets (down to −1.8 °C for Sparsely_treed and − 1.0 °C for Densely_treed). However, the default BEP-Tree simulations seems to capture better the road temperature differences between the two streets at midday (7.4 °C at 11 UTC) with respect to the BEP-Tree w^* simulations (4.4 °C) when they are compared to the observations (9.7 °C).

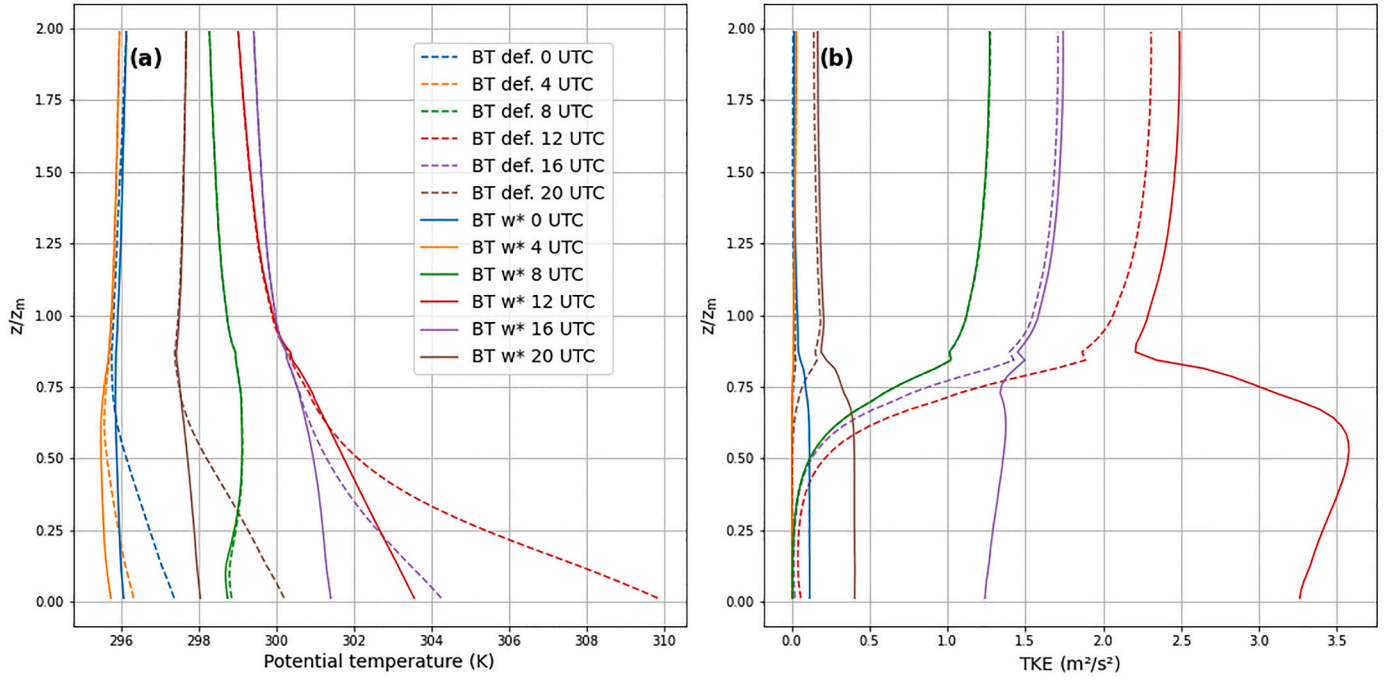

Fig. 3. Vertical profiles of potential temperature (a), and turbulent kinetic energy (b), at 0, 4, 8, 12 16 and 20 UTC for the default BEP-Tree (BT def., dashed lines) and the new BEP-Tree with the thermally driven turbulent wind speed parameterization (BT w*, straight lines) for the Sparsely_treed street. z_m refers to the maximum building height.

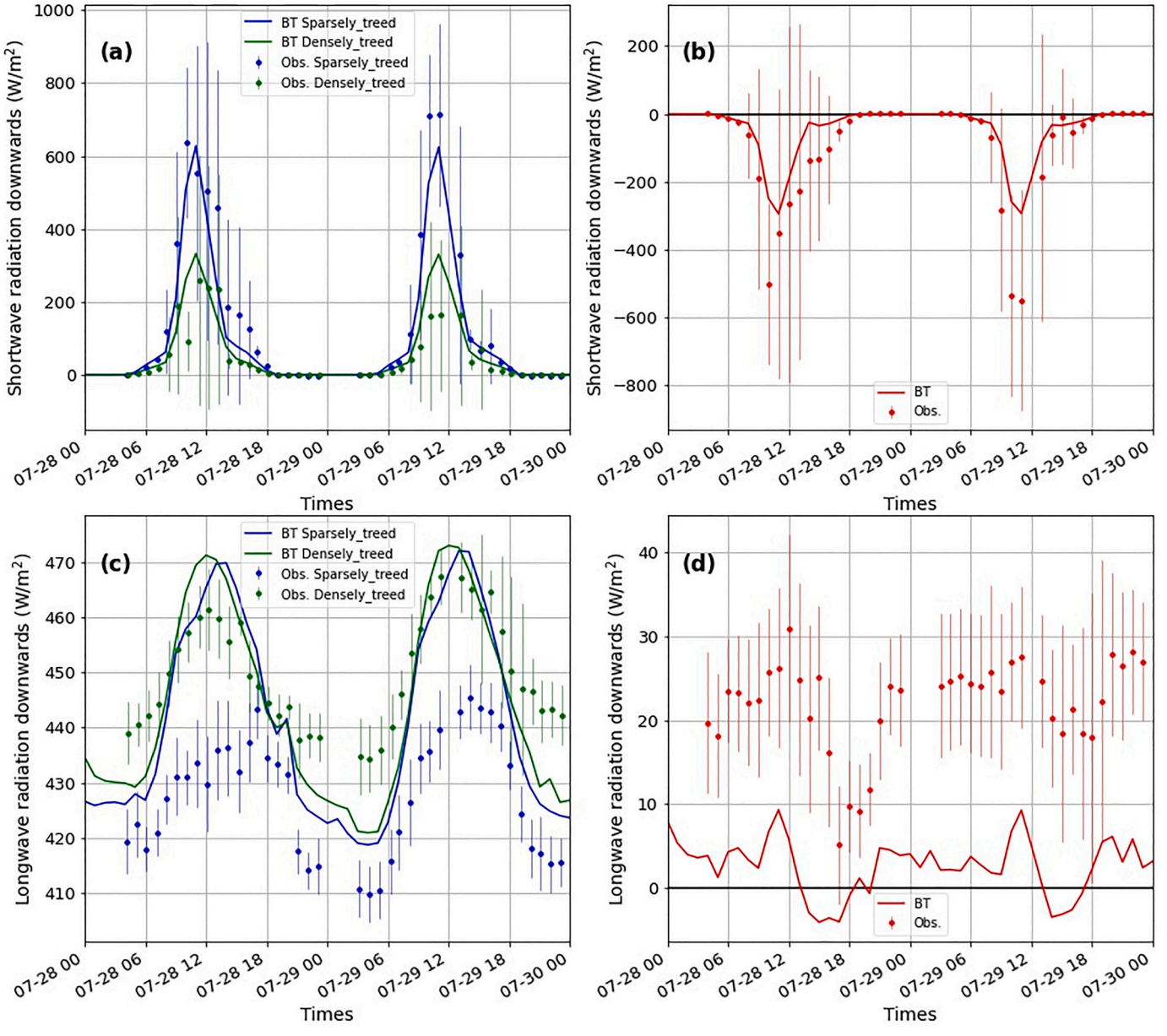

Fig. 4. Modelled by BEP-Tree (BT, lines) and observed (Obs., circles) canyon averaged surface shortwave radiation downwards (a), difference in shortwave radiation downwards between Densely_treed and Sparsely_treed (b), surface longwave radiation downwards (c), difference in longwave radiation downwards between Densely_tree and Sparsely_treed (d) for Sparsely_treed (blue) and Densely_treed (green) streets in Barcelona, and their difference (Densely_treed – Sparsely_treed, red). Measurement error bars correspond to the standard deviation between all the stops. (For interpretation of the references to colour in this figure legend, the reader is referred to the web version of this article.)

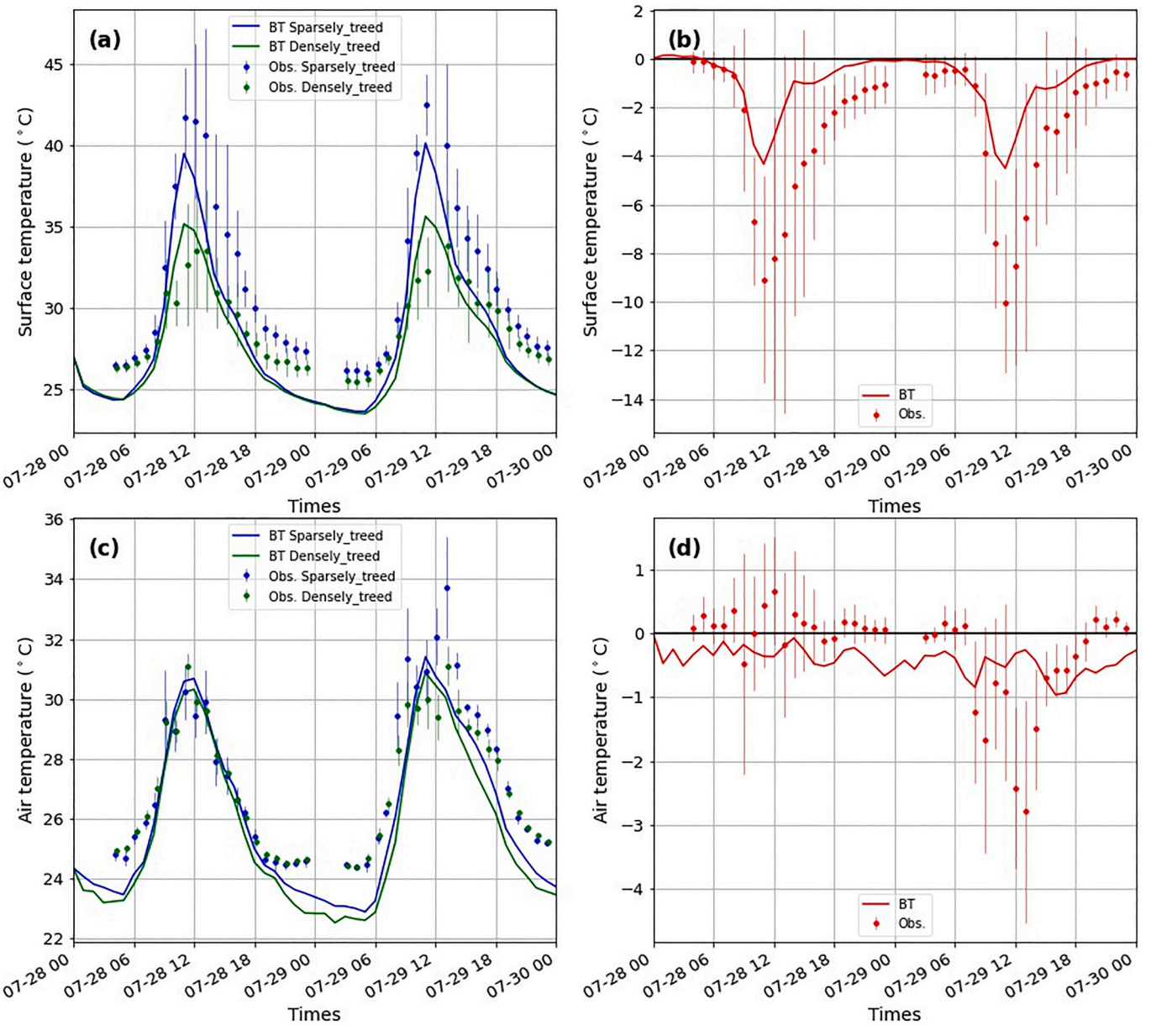

Fig. 5. Modelled by BEP-Tree (BT, lines) and observed (Obs., circles) canyon averaged road surface temperatures (a), difference in road surface temperatures between Densely_treed and Sparsely_treed (b), air temperature (at 1.5 m height from the ground) (c) difference in air temperatures between Densely_treed and Sparsely_treed (d) for Sparsely_treed (blue) and Densely_treed (green) streets in Barcelona, and their difference (Densely_treed – Sparsely_treed, red). Measurement error bars correspond to the standard deviation between all the stops. (For interpretation of the references to colour in this figure legend, the reader is referred to the web version of this article.)

Even though, the inclusion of the thermally driven turbulent wind speed in the model improves the simulation of the road surface temperature diurnal range for the two streets, leaving only a small negative bias in the case of the Sparsely_treed simulation (−2.8 °C).

The inclusion of the thermally driven turbulent wind speed parameterization reduces the simulated maximum air temperatures (up to 6.7 °C compared to BEP-Tree def.) for the two streets despite the enhancement of the sensible heat flux from the ground and walls (Fig. 2b). The enhanced aerodynamic conductance between artificial canyon surfaces and air produces an increment in the turbulent kinetic energy of the entire column, especially during the middle hours of the day, which distributes the added heat from walls and ground to the entire urban canopy via turbulent motions (see Fig. 3b). As with the surface temperature, the air temperature simulated with the default BEP-Tree model presents a higher diurnal range, with much higher maximum values at noon, and similar values at nighttime than the simulations with the modified BEP-Tree. Moreover, the default BEP-Tree model presents a higher cooling rate during the evening and night compared to the simulations with the added thermally driven wind speed and observations, which present almost steady nighttime air temperatures in the two streets. The reduction of the nighttime cooling rate with the new parameterization comes from representing more neutral conditions inside the urban canopy layer compared to the default version of the model (see Fig. 3a) which presents unstable profiles at nighttime.

From now on, only the results of the BEP-Tree model with the new buoyancy driven turbulent wind speed parameterization are compared with the observations.

3.2. Surface radiation downwards

The difference in tree cover density between the two street canyons produces an observed maximum street-level shortwave radiation difference of 550 ± 309 W/m^2 at midday (Fig. 4b). As it was expected, the maximum differences in the shortwave radiation fluxes are observed during the central hours of the day (between 9 and 13 UTC), being over 150 W/m^2 higher for the Sparsely_treed street. During this period, the sun is at its cenital position and sun beams can reach the street ground without obstruction from the canyon buildings. The temporal profiles of the surface shortwave radiation downwards for the two streets follow a similar profile between the two days of the campaign, in agreement with the fact that there were no clouds during the measurement period. The small differences observed in the temporal profiles between the two days are produced by the spatial variability of the random measurement samples.

BEP-Tree presents similar profiles of the surface shortwave radiation downwards for the two streets compared to the observations (Fig. 4a). BEP-Tree estimates a lower shortwave radiation incident to the ground for Sparsely_treed during midday than the measurements (down to −200 W/m^2), especially during the second day. While the model estimates higher incident shortwave radiation at ground level during midday for the Densely_treed case (up to 170 W/m^2) than the measurements. This causes that the modelled differences seen between the two streets are not as high as the ones observed, reaching the downwelling shortwave radiation almost 300 W/m^2 lower for the Densely_treed case.

In the case of the longwave radiation, the measurements exhibit a difference of incoming radiation at street-level of 22 ± 6 W/m^2 higher for the Densely_treed street with respect to Sparsely_treed (Fig. 4d). This difference is kept almost constant during the diurnal cycle between 15 and 30 W/m^2, except during the afternoon hours of the first day (between 17 and 20 UTC), where the difference dropped below 15 W/m^2. Over all the hourly transects, the Densely_treed street presented a higher downwelling longwave radiation at street-level than the Sparsely_treed.

On the other hand, the modelled longwave radiations at ground level presented much smaller differences between the two streets during the campaign period (Fig. 4d). The hourly differences vary between −5 W/m^2 and 10 W/m^2. This discrepancy is produced by the larger longwave radiations estimated for the Sparsely_treed case, compared to the observation, which are between 5 W/m^2 and 35 W/m^2 higher, especially during midday and early afternoon (10–15 UTC). In the case of the Densely_treed street, BEP-Tree estimates lower values during the evening and night than the observations (down to −16 W/m^2), but higher values during midday (up to 10 W/m^2). This causes that the model exhibits negative differences between Densely_treed and Sparsely_treed longwave radiation downwards during the afternoon (between 14 and 18 UTC), in disagreement with the observations, where the differences are always positive.

3.3. Road surface and air temperatures

Road surface temperatures are cooler in Densely_treed than in Sparsely_treed during the whole study period (Fig. 5b), showing maximum differences of 10.1 ± 2.9 °C during midday. Maximum observed road surface temperatures reach up to 42.5 ± 1.9 °C and 33.8 ± 2.8 °C for Sparsely_treed and Densely_treed, respectively. Even during the night, Sparsely_treed exhibits higher surface temperatures than Densely_treed, 1 °C on average during night measurements.

BEP-Tree simulations can capture the daytime effect of trees on the ground surface temperature, showing higher surface temperatures in Sparsely_treed compared to Densely_treed. Even though, the differences between streets are not as wide as in the case of the observations. The maximum difference between streets estimated by the model is 4.4 °C. This low difference of the surface temperature difference between the two streets at midday is related to a lower estimation of the temperatures for the Sparsely_treed street (down to −5.4 °C) and a higher estimation for Densely_treed (up to 3.4 °C). The model estimates lower mid-afternoon and nighttime road surface temperatures for the two streets (around 2.5–3 °C lower for Sparsely_treed and 2 °C lower for Densely_treed) compared to the observations. Moreover, the model is not able to capture the nighttime temperature difference generated by the tree presence, showing identical nighttime surface temperatures between the two streets (differences below 0.3 °C).

The observations of averaged air temperatures in the two streets present a different evolution of the variables for the two days of the

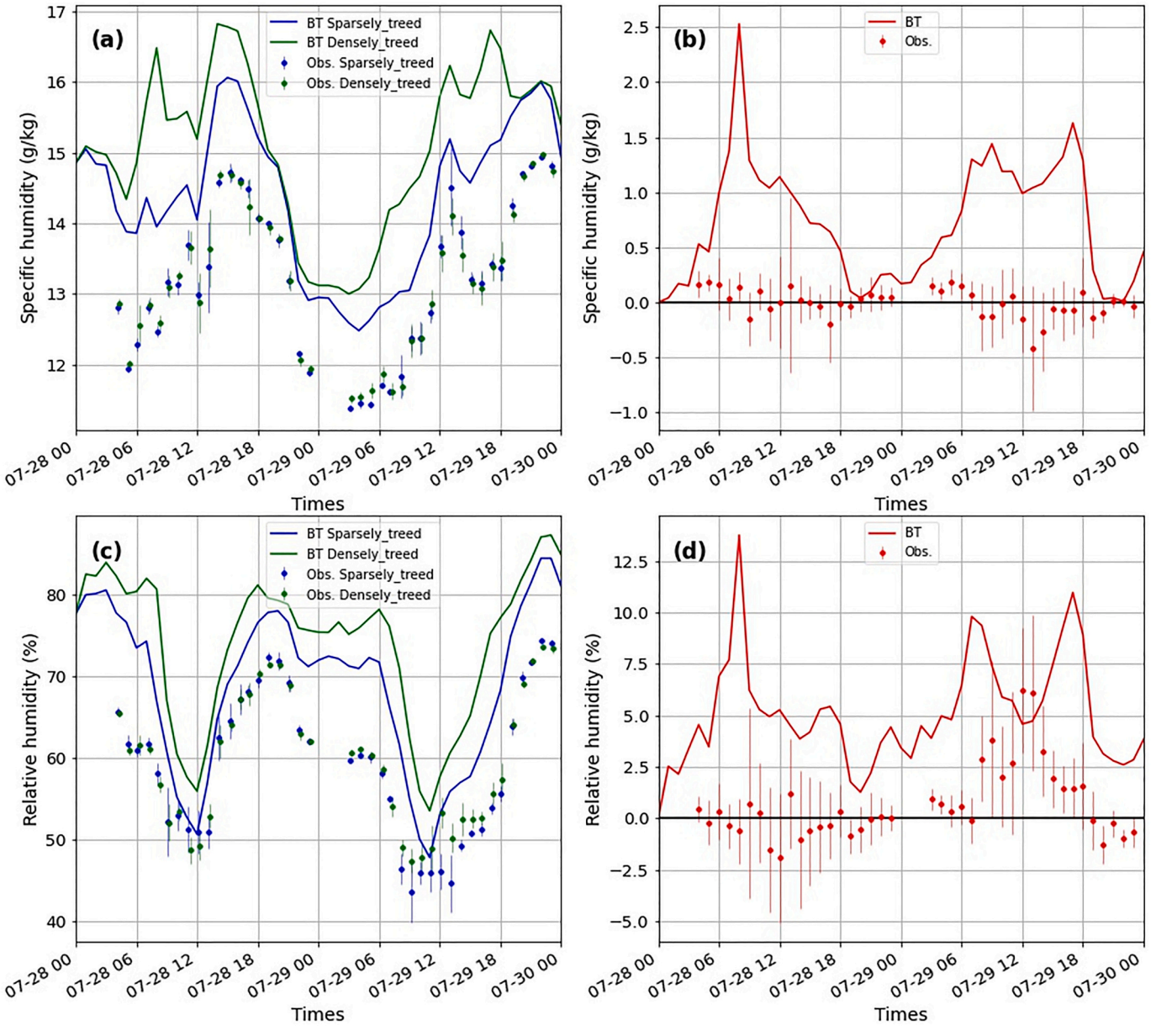

Fig. 6. Modelled by BEP-Tree (BT, lines) and observed (Obs., circles) canyon averaged 1.5 m above ground specific humidity (a), difference in specific humidity between Densely_treed and Sparsely_treed (b), relative humidity (c), difference in relative humidity for Sparsely_treed (blue) and Densely_treed (green) streets in Barcelona. Measurement error bars correspond to the standard deviation between all the stops. (For interpretation of the references to colour in this figure legend, the reader is referred to the web version of this article.)

campaign (Fig. 5c). In the case of the 28 of July, the two streets show a similar evolution of the air temperature, reaching maximum values of 31.1 ± 0.4 °C for Densely_treed and 30.2 ± 0.9 °C for Sparsely_treed at 11 UTC. On the contrary, for the 29 of July, the street with lower tree cover density considered higher averaged air temperatures with maximum values of 33.7 ± 1.7 °C compared to the maximum temperatures of Densely_treed of 31.1 ± 0.7 °C. The average difference in air temperature between the two streets during midday and afternoon of the second day (from 8 UTC to 17 UTC) is 1.3 °C. At nighttime, there is not an observable air temperature difference between the two streets.

BEP-Tree simulations can represent the daytime evolution of the air temperature in the two streets, although an underestimation of the air temperature is observed during the nighttime (Fig. 5c). The model represents lower nighttime air temperatures for the two streets compared to the observations, by 1.8 °C for Sparsely_treed and 1.5 °C for Densely_treed. Model simulations represent higher daytime temperatures for Sparsely_treed compared to Densely_treed for the two days of study. This contrats with the results of the measurements, where Densely_treed exhibits generally slightly higher air temperatures (up to 0.7 ± 0.8 °C) during day 28 of July, while it presents lower temperatures during midday and afternoon of 29 of July (down to −2.8 ± 1.7 °C). Contrasting with the observations, the higher differences between the streets are simulated during mid-afternoon (15–17 UTC) with maximum differences of up to 1.0 °C, compared with the observations which the maximum differences are seen at midday of the second day (11–14 UTC).

3.4. Relative humidity and specific humidity

Our observations do not show a significant difference in specific humidity between the two streets (Fig. 6a). The observed differences between Densely_treed and Sparsely_treed are kept between 0.2 g/kg and − 0.5 g/kg. In the case of the relative humidity, a slight increase of 6.2 ± 3.0% in Densely_treed with respect to Sparsely_treed is observed at noon of the 29 of July (Fig. 6b), corresponding to the decrease of temperatures by the street trees observed in Fig. 5d.

On the contrary, BEP-Tree simulations present a difference in specific humidity between the two streets. This difference is principally appreciable during the daytime, with the simulation with higher tree cover reaching up to 2.5 g/kg more than for Sparsely_treed. This higher difference modelled by BEP-Tree compared to the difference seen in the observations is produced by a higher estimation of the specific humidity in the Densely_treed street. The model is closely representing the evolution of the specific humidity for the Sparsely_treed street with a consistent positive difference, caused by the similar temporal profile between the observations and the specific humidity forcing conditions in the forcing level (see Fig. S5 in the Supplementary material). In the case of the relative humidity, the model is overestimating the differences between the two streets (up to 14% difference between Densely_treed and Sparsely_treed), probably related to the differences seen in the specific humidity during the day, and of the specific humidity and temperature during the night (Fig. 5d).

4. Discussion

4.1. Sensitivity analysis to the wind parameterization

Based on the results of the sensitivity analysis, the new parameterization improves the performance of the model in the representation of street-averaged surface temperatures, decreasing the maximum overestimation during midday (from 7.0 °C to 5.4 °C for Sparsely_treed, and from up to 9.7 °C to 3.4 °C for Densely_treed), and decreasing the cooling rate during the night. Moreover, the buoyancy driven wind velocity parameterization decreases the overestimation of midday air temperatures (from 7.9 °C to −3.4 °C for Sparsely_treed, and from up to 6.3 °C to 1.1 °C for Densely_treed), along to a decrease in the air cooling rate at night, as it is observed from the measurements. It also results in an increment of the TKE inside the canyon. We do not have experimental evidence to assess if this increment is realistic or not, and it is beyond the scope of the present article. To check it, a detailed field campaign should be organized with sonic anemometers located at different heights within the canyon, or a Large Eddy Simulation in non-neutral conditions with surface heat forcing similar the one observed in this case, and the same canyon aspect ratio should be performed.

4.2. Comparison of observations and BEP-tree simulations

4.2.1. Radiation fluxes

The main mechanism that induces local thermal cooling from street trees derives from the shading of ground surfaces, especially artificial materials such as asphalt and concrete which have high heat retention, and the corresponding redirection of sensible heat into latent heat via transpiration. The random location of the stops made by the measurement vehicle in the two traffic lanes of each street provides sufficient sampling to capture the spatial variability of building and tree shade, which increases the standard deviation of the measurements observed from the pyranometer. BEP-Tree is able to capture the daily evolution of ground incident shortwave radiation, while it estimates a lower reduction from the interception by the tree canopies in each street than the observations. BEP-Tree estimates a lower downwelling shortwave radiation at ground level at Sparsely_treed street than the observations during midday (down to −200 W/m^2), while BEP-Tree considers a higher downwelling shortwave radiation for Densely_treed (up to 170 W/m^2). This lower simulated radiation in Sparsely_treed could be related to the spatial discrepancy between the measurements and the simulations. The measurements were taken in the middle of the street where a higher amount of sunlight is reaching the surface, away from the tree cover, which is mostly covering the sidewalks near the walls. This contrasts with the results of the model, which considers the street average surface radiation downwards, including the street sections with shading from tree cover. The higher simulated values than the observations in Densely_treed could be explained because BEP-Tree model is overestimating the SVF for this street in detriment of a

lower BVF as seen in Table 1. This causes that the difference in SVF between the two streets is lower in the model, which produces lower differences in the modelled shortwave radiation downwards. Or it could simply be the result of the observations being taken under the densest part of the tree foliage, while BEP-Tree assumes that the foliage is equally likely to be located above any part of the street.

Despite the interception of direct shortwave radiation that can improve the biometeorological conditions of the pedestrian-level climate, street trees can make the perceived thermal comfort by pedestrians somewhat worse, especially at night, due to the higher emission of longwave radiation from the relatively warm tree leaves compared to the relatively colder sky that the vegetation obscures. The reduction of the SVF by street trees means that a higher proportion of the longwave radiation released by the warm street ground and walls is absorbed and reemitted back to the ground by the vegetation. This effect can be seen in the measurements (Fig. 4d) in which exhibit a difference of incoming longwave radiation at street level of 22 $\pm$ 6 W/m^2 higher for the Densely_treed street with respect to Sparsely_treed. The BEP-Tree model predicts a small increase of incident longwave radiation to the street during midday and nighttime as a result of tree foliage blocking the relatively cool sky (however, in the afternoon it also blocks hot walls, causing reduced street level incoming longwave). The fact that the model is simulating the downward longwave radiation to the whole canyon ground, while the measurements only capture the radiation incident to the central portion of the canyon, leads to the model seeing a higher portion of the building walls than the measurements. This discrepancy affects principally the comparison between the model and the measurements in Sparsely_treed, which has lower tree cover, because the model computes a higher BVF for this street (0.613) compared to Densely_treed (0.374). Moreover, the model calculates a lower BVF for Densely_treed and a larger SVF than the one observed, which reduces even more the downwards longwave radiation from this street. This effect principally occurs during afternoon, due to the higher difference in temperature between the building walls and the sky or trees, likely causing that Sparsely_treed presents higher downwelling longwave radiation than Densely_treed in the model.

4.2.2. Road surface and air temperatures

Street trees produce a decrease in road surface temperatures due to the shading, while they can increase surface temperatures by the higher incident longwave radiation and the reduced street-level wind flow from the larger roughness elements, which lowers the heat flux transfer from ground to the air (Coutts et al., 2016; Krayenhoff et al., 2020). From the measurements it can be seen that street trees decrease road surface temperatures (Fig. 5a), showing maximum differences of 10.1 $\pm$ 2.9 °C during midday. Even during the night, the Sparsely_treed street surface exhibited higher temperatures than Densely_treed, likely indicating that the reduction of the thermal load accumulated in the asphalt from the tree shading was greater than the longwave and wind drag effects induced by trees that serve to increase street surface temperatures. BEP-Tree simulations can capture the daytime effect of trees on the ground surface temperature, showing higher surface temperatures in Sparsely_treed of up to 4.5 °C. This underestimation of the surface temperature difference between the two streets at midday can be related to the differences seen in the shortwave radiation downwards between the observations and BEP-Tree (Fig. 4b), which are in part related to the difference between point observations and the spatially-averaged model results. The model underestimates the mid-afternoon and nighttime road surface temperatures for the two streets. Moreover, the model is not able to capture the nighttime temperature difference generated by the tree presence, showing identical nighttime surface temperatures between the two streets. The SVF differences between the two streets are not as large in the 'spatially-averaged' model

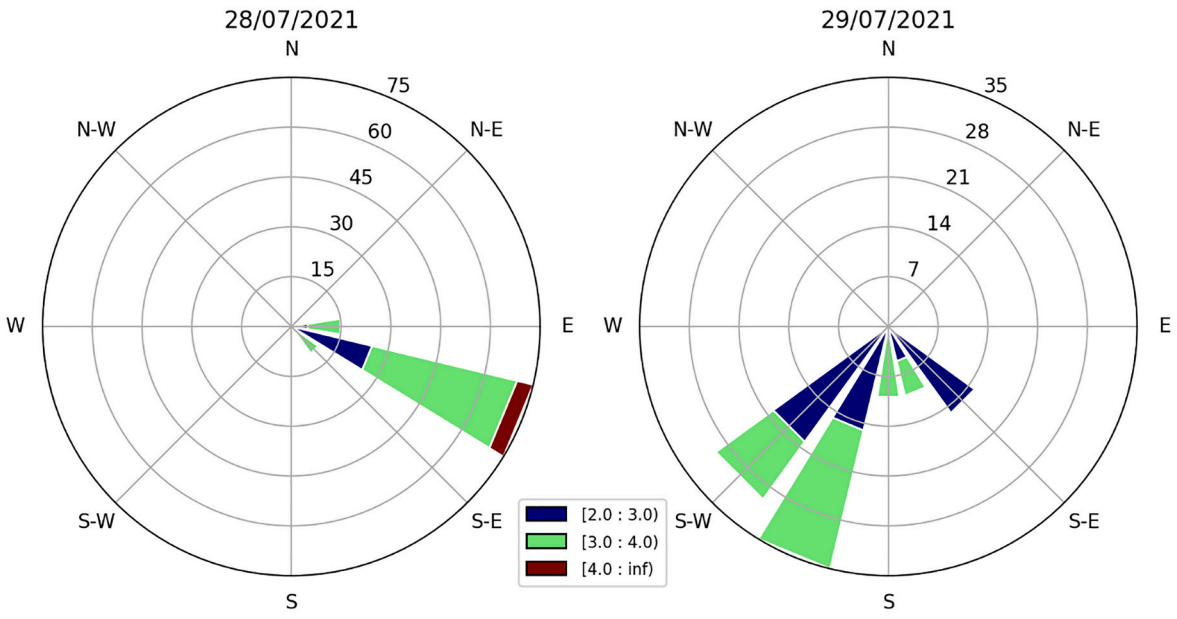

Fig. 7. Windrose in percentage (%) of the two days of campaign during the central hours of the day (8 UTC - 17 UTC) measured at the Raval meteorological station. The streets studied are oriented from NW to SE.

compared to the 'point' observations (see Table 1), which can reduce the difference in the radiative cooling of the canyon surfaces.

Air temperatures can be affected at neighborhood scales by street trees due to the reduction of ground and wall surface temperatures and the corresponding reduction of sensible heat transmitted from the shaded surface to the air. Nevertheless, the effects of street trees can be suppressed by the local meteorological conditions. For example, periods of high wind speed can produce lower effects of trees on the air temperatures if the wind blows in the same direction of the street due to the advection of the cooling effects downstream (Oke, 1989). The observations of averaged air temperatures in the two streets present a different evolution of the variables for the two days of the campaign (Fig. 5c). The differences observed between the two days could be related to the local wind direction. On the 28 of July, the wind flows principally from the coast coming from ESE (Fig. 7), which is almost in the same direction as the street orientation. In this situation, wind flow can be channeled through the street canyons, advecting air masses from upwind locations of the city and suppressing the possible effects of streets trees on the air temperature. This can likely explain the low observed difference in air temperature between the two streets during this day (0.7 ± 0.8 °C higher for Densely_treed). On the contrary, the wind flow mainly from SW and SSW on the second day of campaign (Fig. 7), perpendicular to the street orientation. This causes less ventilation inside the deepest part of the canyons and the air exchange between the urban canopy layer and the free atmosphere above roof level was probably reduced (Oke et al., 2017). In this situation, the cooling effect of street trees shading on the ground is likely enhanced due to the reduced wind speed near the ground (Lin and Lin, 2010). This could explain the high temperature differences observed for this day (up to 2.8 ± 1.7 °C higher for Sparsely_treed). However, even though the cooling effect of street trees is likely maximized during this wind direction, the dispersion of air pollution can be severely worsened during these situations, due to the stagnation of air pollutants inside the street canyon (Oke et al., 2017), especially if street trees are present, because they serve to further disconnect the wind flow above the canyon from that under the tree canopy (Jin et al., 2014; Janhäll, 2015).

The results have shown that BEP-Tree can represent the daytime evolution of the air temperature in the two streets, although an underestimation of the air temperature is observed during the nighttime (Fig. 5c). This underestimation of nighttime temperatures could be in part explained by the emission of anthropogenic heat sources inside the canyon, not considered by the model. The high presence of traffic inside the two canyons during the day until after sunset, combined with the release to the canyon air of residual heat from building air conditioning systems can be a non-negligible factor in the evolution of the air temperature inside the urban canopy layer, especially in deep and narrow canyons (Huang et al., 2020) and during nighttime when mixing is reduced. Another possible explanation could be an underrepresentation of the heat storage in the street ground by the model which limits the amount of heat released at nighttime. The heat storage depends on the inner temperatures of the building and ground surfaces, as well as the material properties, which are highly uncertain and difficult to measure.

Model simulations represent higher daytime temperatures for the Sparsely_treed site compared to the Densely_treed site for the two days of study. BEP-Tree is unable to detect the differences in air temperature of the two days of study due to the different wind regime inside the urban canyons. BEP-Tree does not explicitly resolve the effect of above roof wind direction inside the streets canyons because it is designed to compute the neighborhood average urban canopy layer behavior, considering the average variables between the two street orientations. In this case, since the simulations only consider one street orientation, we can account for the effects of street orientation on the solar radiation, but not the effects of above roof wind direction and neighborhood-city scale wind circulations. Future studies should focus on determining the impact of above-roof wind direction on the urban canopy layer, in order to estimate how this factor affects the air cooling of street trees.

4.2.3. Relative humidity and specific humidity

Street trees can produce a reduction of air temperature through transpiration, which is the transformation of sensible heat into latent heat, releasing water vapor into the air (Bowler et al., 2010). This process produces an increment of the relative humidity and specific humidity in the canyon. However, our observations do not show a significant difference in specific humidity between the two streets (Fig. 6a). This could be explained by three reasons. The first one is that the meteorological device used in the measurements requires a longer time to reach the equilibrium conditions with the surrounding air in the case of relative humidity compared to air temperature and radiation fluxes. This can result in an inability of the device to determine the difference in the two streets if the time to complete an entire track is shorter than the response time of the device (around 20 min for the relative humidity). The second reason could be that leaf transpiration can be suppressed due to water scarcity in the soil (Vico et al., 2014), increased air temperature, and/or photoprotection of the photosystem from excess of light (Galmés et al., 2011). During the measurement campaign, there were extremely dry conditions in the city, and it was combined with high solar exposition of the vegetation. This drought situation is combined with the high imperviousness of urban surface covers, which increase the water runoff and decrease the accumulation of water in inner soil layers. The net result is that street trees lack water at the root levels to perform the leaf transpiration, deriving in stomatal closure and producing similar specific humidity in the two streets. The third reason is that neighborhood scale advection may have caused sufficient mixing to suppress humidity differences between the streets.

Contrasting with the results, BEP-Tree simulations present a difference in specific humidity between the two streets that can be appreciated better during the daytime. This discrepancy with the observations can be produced due to the long response time of the meteorological device used in the campaign or because BEP-Tree model is not including ecophysiological responses of the vegetation to soil hydrology. In the current version of BEP-Tree there is no soil water dynamics and in the current application the term that controls the stomatal opening related with soil moisture is set to 1.0 (see eq. 14 in Krayenhoff et al., 2020), such that trees do not experience water scarcity. This simplification of soil hydrology can affect estimation of the effects of trees on street microclimate in periods of severe drought, as in the one studied.

4.2.4. Model vs observations discrepancies

The observational campaign described in this study has been designed to evaluate the BEP-Tree model for the highly compact city of Barcelona. Due to the considerable limitations of performing a micrometeorological campaign in a highly dense city, vehicle transects were conducted inside one of the densest and most urbanized neighborhoods of Barcelona. Although this methodology allows sampling of the variability of building and tree shading along the street's direction, this strategy limits sampling to the traffic lanes, and it is not able to capture the microclimatic conditions in the sidewalks, where pedestrians circulate. This contrasts with the street-average microclimate simulated with BEP-Tree, which represents the average climate over the full canyon width. This difference in spatial representation/sampling generates minor discrepancies between observed and modelled downwelling shortwave radiation (Section 3.2.) and road surface temperature (Section 3.3.), and larger discrepancies between observed and modelled downwelling longwave radiation (Section 3.2.).

Moreover, street trees are usually placed near the sidewalks, in order to maximize the shading to the pedestrians. This affects principally the comparison of the measurements and BEP-Tree simulations in the Sparsely_treed street, where trees are covering principally the sidewalks, while for Densely_treed they cover fully the canyon width, including the traffic lanes. While vehicle radiation measurements were not able to capture the shading from Sparsely_treed trees, BEP-Tree simulations considered tree shading because trees are randomly distributed over the street canyon in the model. Future observational micrometeorological studies may combine the vehicle measurements in the central portion of the street with a mobile human-biometeorological station such in Middel and Krayenhoff (2019) for the sidewalks, so as to determine the average effect of street trees in the whole canyon.

Overall, there is a good agreement in the comparison between the microclimatic effect of street trees observed in the campaign and modelled with BEP-Tree, considering the limitations associated with simulating the complex microclimate observed inside deep urban canyons with street trees; and the spatial discrepancies between point measurements and spatially-averaged model output. Moreover, while BEP-Tree effectively assumes the whole neighborhood has the characteristics of the single canyon modelled here (or of two canyons of different orientation in its typical implementation), in reality the air temperature and humidity are determined by the characteristics beyond the individual canyon. BEP-Tree is designed to be coupled with a mesoscale model which in turn provides horizontal advection above and within the urban canyon. In standalone (offline) mode, as it is used in this study, BEP-Tree cannot capture horizontal temperature and humidity advection which may play a role in the discrepancies observed in this study, i.e. the underestimation of nighttime air temperatures or the discrepancy observed in the specific humidity. Even though, the regular building pattern and similar building height of the study area along to the identical morphology conditions in the entire neighborhood facilitates the representation of the actual conditions inside the canyons by the model, and probably explains the good performance of the model representing the daytime air temperatures or the specific humidity in the Sparsely_treed street. Further studies can be centered on the evaluation of BEP-Tree coupled with a mesoscale model in order to consider the possible impacts of horizontal advection of air temperature and humidity, along to study the impacts of street trees in other regions of the city, i.e. regions with more complex street patterns and even higher packing densities such as those observed in the second most dominant geometry of the city (see Section 2.2.1).

Larger differences between simulated and observed air and surface temperature are seen at night, which can be attributed to the lack of representation of anthropogenic heat source in the model or due to potential inaccuracies in the representation of the heat storage in street surfaces. Highly-compact areas such the studied area in Barcelona have high emissions of anthropogenic heat from vehicles and residual heat from building air conditioning systems (Gilabert et al., 2021), which can be an important component in the overall energy balance of the urban canopy layer (Oke et al., 2017). Future evaluations of BEP-Tree model in high-dense cities must consider the contribution of anthropogenic heat sources in the local climate of the street's canyons, such as including a building energy model as the Building Effect Parameterization and the Building Energy Model (BEP-BEM) (Salamanca and Martilli, 2010) and including additional inventoried traffic emissions in the lowest vertical levels.

4.3. Effect of street trees on thermal comfort

Keeping in mind the limitations of the model, in this section we investigate the impact of trees on thermal comfort. The results shown indicate that street trees modify the microclimate inside the urban canyon, producing a clear effect on radiation and air temperature. These effects can change the biometeorological conditions perceived by a pedestrian in these streets. Human thermal comfort can be estimated by the human heat budget, as many thermophysiological assessment indices do (Mayer and Höppe, 1987; Jendritzky et al., 2012). These indices are estimated principally from the meteorological conditions surrounding the pedestrian, i.e. the air temperature, water vapor pressure, wind velocity and the mean radiant temperature (T_{mrt}), which is defined as the uniform temperature of an imaginary sphere surrounding a human body in which the radiant heat transfer from the body to the enclosure is equal to the radiant heat transfer to the actual non-uniform surrounding (ISO, 1998; Thorsson et al., 2007). The mean radiant temperature accounts for the combination of shortwave and longwave radiation fluxes perceived by the human body at the 3 spatial dimensions. Although it is not in the scope of this study to quantify the effect of street trees on the thermal comfort for high-compact cities, we can make some estimates of the overall changes in thermal comfort produced by street trees based on the changes in the air temperature, radiation fluxes and humidity from the observations and BEP-Tree simulations.

Based on the observations of air temperatures between Densely_treed and Sparsely_treed streets, the increase in the tree cover density reduces or slightly increases the air temperature dependeing on the local meteorological conditions. As it is seen in the second day of campaign, the reduction of air temperature at noon in Densely_treed is expected to improve the thermal comfort at noon with respect to the conditions in Sparsely_treed. On the contrary, on the first day of campaign there is a nonsignificant increase of temperatures that could slightly worsen the felt conditions. In contrasts with the results of other observational studies which observe an

increase in nighttime temperatures due to the presence of street trees (Taha et al., 1991; Bowler et al., 2010), in our case there is no increase in night air temperatures due to the increased tree cover, which implies that there is no worsening of the thermal comfort associated to the effect of street trees on the air temperature.

In terms of radiation fluxes, the presence of street trees reduces the downwelling shortwave radiation (see Section 3.2.). Moreover, tree shading reduces the road surface temperatures based on the observations and the BEP-Tree model (Fig. 5b), implying a reduction of the longwave radiation emitted from the ground upwards. Recent modelling work indicates that reduced longwave emission toward pedestrians due to tree shade may account for >25% of the reductions in T_{mrt} associated with trees (Lachapelle et al., 2022). Additionally, the comparison of the building wall temperatures from the simulations reveals that the higher tree cover in Densely_treed generates a lower building wall temperature in the lowest levels compared to Sparsely_treed (see Fig. 8). This turns up into a lower emission of longwave radiation from the walls to the pedestrians, which decreases T_{mrt}.

However, the higher tree cover has been shown to increase the emission of downwelling radiation from the reduction of the SVF (Krayenhoff et al., 2020), which can counteract the reductions in T_{mrt} from the increased shading on ground and walls. Nevertheless, based on the sum of the longwave radiation upwards and downwards to the street surface in the model, and at 1.5 m above the ground from the observations (Fig. 9), during daytime the street with lower tree cover density has higher exposure to longwave radiation. Therefore, we can assert that street trees will imply a significant reduction of the mean radiant temperature at noon. On the contrary, at nighttime, the comparison between streets of the sum of longwave radiation fluxes in the two vertical directions reveals that the higher tree cover density produces a higher exposure to longwave radiation near the ground surface (Fig. 9). Considering that the wall surface nighttime temperatures are similar between the two simulations (Sparsely_treed and Densely_treed), we concur that trees do not reduce the lateral longwave radiation perceived by the pedestrian. As seen by other authors (Middel and Krayenhoff, 2019) this finding implies that the mean radiant temperature will increase with the presence of trees due to the enhanced vertical longwave radiation exposure at pedestrian level.

Based on the findings of previous studies in hot, dry conditions (Middel and Krayenhoff, 2019), the thermophysiological assessment indices are more sensitive to variations of air temperature and mean radiant temperature than to wind speed or relative humidity. Therefore, we can posit that street trees improve daytime thermal comfort in deep canyons, especially when above-roof wind direction is perpendicular to the streets orientation, based on the reductions observed of air temperature and the assumed reduction of the mean radiant temperature deduced from the observations and the BEP-Tree simulations. On the contrary, during the evening and nighttime, air temperatures and wall temperatures do not present a significant difference between the two streets, and the downwelling longwave radiation increases due to the obscuration of the sky by tree leaves, indicating that street trees are likely to worsen thermal conditions slightly.

These assumptions agree with the results of several microclimatic studies centered in the cooling effect of street trees (Coutts et al., 2016; Middel and Krayenhoff, 2019). Coutts et al. (2016) concluded that street trees can lower the heat stress at daytime during extreme heat events over the city of Melbourne (Australia) principally to the reduction of T_{mrt}, rather than air temperature. Moreover, they observed a slight increase at night in the T_{mrt} and UTCI due to the increased tree cover density. Middel and Krayenhoff (2019) observed that tree canopies were able to significantly reduce the T_{mrt} for an extremely hot day in Tempe (Arizona) with maximum reductions up to 33.4 °C, although a warming effect was also seen in the measurements under trees made after sunset of about 5 °C. Nevertheless, the effect of street trees on human biometeorology are determined by the local meteorological conditions, the urban geometry and cover and the tree cover density (Shashua-Bar et al., 2011; Coutts et al., 2016). Future improvements in BEP-Tree model can focus on the development of the mean radiant temperature calculation inside the urban canyon in order to allow the model to further derive thermophysiological assessment indices. This implementation would be useful to further study the impact of street trees in the thermal comfort under the different conditions previously mentioned.

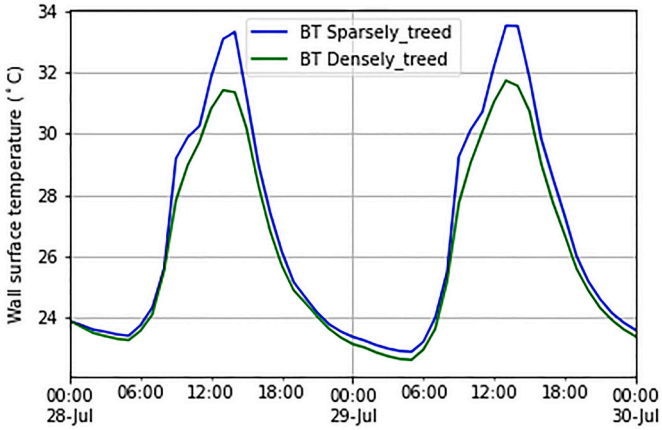

Fig. 8. Modelled surface wall temperatures averaged between the two sides of street canyon and the first 10 m of altitude, representing the building wall surfaces below the maximum tree height in the Densely_treed street.

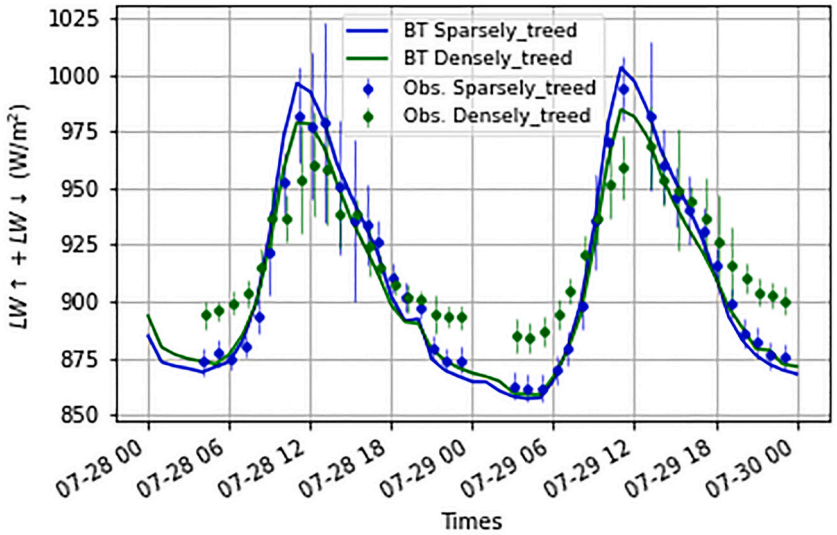

Fig. 9. Modelled by BEP-Tree (BT, at ground surface) and observed (Obs., at 1.5 m above the ground) sum of upwelling and downwelling longwave radiation for Sparsely_treed (blue) and Densely_treed (green) streets. (For interpretation of the references to colour in this figure legend, the reader is referred to the web version of this article.)

5. Summary and conclusions

In this study, a neighborhood-scale urban canopy model that integrates the effects of street trees on the street microclimate is evaluated and improved for the highly-compact city of Barcelona, Spain. BEP-Tree model simulations of two parallel streets with high and low tree cover densities are compared against observations of a micrometeorological measurement campaign performed in the area for two summer days. During the campaign, hourly vehicle transects were performed in the two streets measuring vertically-oriented shortwave and longwave radiation fluxes, air temperature and humidity. The measurement period spanned from before sunrise to long after sunset to capture the evolution of the street microclimate along the diurnal cycle. The regular building pattern and the identical urban morphology along the entire neighborhood of the study area, allowed a better representation of the observed canyon-averaged climate and radiation fluxes by the BEP-Tree model.

We have presented a new turbulent wind speed parameterization included in the BEP-Tree model to solve the inefficient modelled heat exchange between urban surfaces and the air in the lowest levels of the deep street canyons. We have defined a new buoyancy driven turbulent vertical wind velocity w^*(see Eq. (3)) to consider non-negligible buoyancy production of turbulence inside the canyon for unstable conditions. BEP-Tree simulations with the new parameterization show a higher aerodynamic heat conductance between ground surface and air, improving the simulation of surface temperatures. Moreover, the new parameterization also reduces pedestrian-level air temperatures during daytime from the enhancement of the turbulent kinetic energy inside the canyon, improving the representation of air temperatures and buoyancy mixing in the urban canopy layer.

The observations evidenced that street trees contribute to the regulation of the climate inside the canyons through shading of urban surfaces. BEP-Tree simulations were able to reproduce the observed reduction of shortwave radiation through leaf interception and the reduced road temperature derived from the lower irradiance reaching the street surface. Moreover, an increment of the downwelling longwave radiation is observed (modelled) at pedestrian-level (ground level) explained by the higher canopy temperature compared to the relative cool sky that the leaves obscure. Based on the differences observed in air temperatures between the two days of the campaign we can conclude that the effect of street trees in air temperatures is highly dependent on the local meteorological conditions, such as the wind direction above the urban canopy layer. During the first day of campaign, we observed similar daytime air temperatures between the two streets, coinciding with the above roof wind blowing in the same direction as the orientation of the streets being measured and modelled. Wind blew perpendicular to the direction of the streets of interest on the second day of the campaign, and the air temperature in the street with lower tree cover density was 1.3 °C higher on average compared with the street with higher tree cover density. BEP-Tree simulations were able to closely capture the daily evolution of air temperatures with a modest negative bias during nighttime. However, BEP-Tree was not able to capture the differences in the effects of street trees with the above wind direction because it does not capture the effects of sub-neighborhood scale horizontal heterogeneity.

Finally, based on the modelled and observed effects of street trees on the street microclimate we discuss the possible impacts of street trees on the thermal comfort during hot, dry conditions in a highly-compact urban neighborhood. Street trees are expected to improve the thermal comfort during daytime, due to the reduction of the mean radiant temperature through shortwave radiation interception and reduced emission of longwave radiation from the canyon surfaces due to the lower surface temperatures. On the contrary, at night the higher presence of street trees is expected to create minor thermal discomfort due to higher emission of longwave radiation downwards. BEP-Tree can be an adequate tool to perform these studies since it incorporates a reliable representation of the

effect of street trees on the street climate and radiation. Further implementations in BEP-Tree should focus in integrating the mean radiant temperature calculation in the model, in order to assess all the meteorological forcings that drive influence in the thermal comfort during hot and dry periods.

Code and data availability

The version of the BEP-Tree code and the datasets generated during and/or analyzed during the current study are available from the corresponding author on reasonable request.

Funding

Gara Villalba reports financial support was provided by European Research Council.

Declaration of Competing Interest

The authors declare that they have no known competing financial interests or personal relationships that could have appeared to influence the work reported in this paper.

Data availability

Data will be made available on request.

Acknowledgements

This study has been carried out thanks to the financial support of the ERC Consolidator Integrated System Analysis of Urban Vegetation and Agriculture (818002-URBAG). The authors would also like to thank the support of the Spanish Ministry of Science, Innovation and Universities, through the “Maria de Maeztu” programme for Units of Excellence (CEX2019-000940-M), as well as a Discovery Grant from the Natural Sciences and Engineering Research Council of Canada. The authors thankfully acknowledge the computer resources at PICASSO and the technical support provided by the Universidad de Málaga (RES-AECT-2020-2-0004). Sincere thanks to the Universitat Pompeu Fabra of Barcelona for the permission to install the meteorological station in their building rooftop.

Appendix A. Supplementary data

Supplementary data to this article can be found online at https://doi.org/10.1016/j.uclim.2022.101288.

References

Arnfield, A.J., 2003. Two decades of urban climate research: a review of turbulence, exchanges of energy and water, and the urban heat island. Int. J. Climatol. 23 (1), 1–26. https://doi.org/10.1002/joc.859.

Barcelona City Council Statistical Yearbook, 2021. Department of Statistics, Barcelona City Council, Barcelona, Spain. Retrieved from. bcn.cat/estadistica.

Baró, F., Calderón-Argelich, A., Langemeyer, J., Connolly, J.J.T., 2019. Under one canopy? Assessing the distributional environmental justice implications of street tree benefits in Barcelona. Environ. Sci. Pol. 102, 54–64. https://doi.org/10.1016/j.envsci.2019.08.016.

Bowler, D.E., Buyung-Ali, L., Knight, T.M., Pullin, A.S., 2010, September. Urban greening to cool towns and cities: a systematic review of the empirical evidence. Landsc. Urban Plan. https://doi.org/10.1016/j.landurbplan.2010.05.006.

Coutts, A.M., White, E.C., Tapper, N.J., Beringer, J., Livesley, S.J., 2016. Temperature and human thermal comfort effects of street trees across three contrasting street canyon environments. Theor. Appl. Climatol. 124 (1–2), 55–68. https://doi.org/10.1007/s00704-015-1409-y.

Demuzere, M., Orru, K., Heidrich, O., Olazabal, E., Geneletti, D., Orru, H., Faehnle, M., 2014. Mitigating and adapting to climate change: multi-functional and multi-scale assessment of green urban infrastructure. J. Environ. Manag. 146, 107–115. https://doi.org/10.1016/j.jenvman.2014.07.025.

Galmés, J., Flexas, J., Medrano, H., Niinemets, Valladares, F., 2011. Ecophysiology of photosynthesis in semi-arid environments. In: Terrestrial Photosynthesis in a Changing Environment a Molecular, Physiological and Ecological Approach. Cambridge University Press, pp. 448–464. https://doi.org/10.1017/CBO9781139051477.035.

Gilabert, J., Ventura, S., Segura, R., Martilli, A., Badia, A., Llasat, C., Corbera, J., Villalba, G., 2021. Abating heat waves in a coastal Mediterranean city: what can cool roofs and vegetation contribute? Urban Clim. 37 https://doi.org/10.1016/j.uclim.2021.100863.

Gillner, S., Vogt, J., Tharang, A., Dettmann, S., Roloff, A., 2015. Role of street trees in mitigating effects of heat and drought at highly sealed urban sites. Landsc. Urban Plan. 143, 33–42. https://doi.org/10.1016/j.landurbplan.2015.06.005.

Grimmond, C.S.B., Oke, T.R., 1991. An evapotranspiration-interception model for urban areas. Water Resour. Res. 27 (7), 1739–1755. https://doi.org/10.1029/91WR00557.

Grimmond, C.S.B., Oke, T.R., 1999. Aerodynamic properties of urban areas derived from analysis of surface form. J. Appl. Meteorol. 38 (9), 1262–1292. https://doi.org/10.1175/1520-0450(1999)038<1262:APOUAD>2.0.CO;2.

Grimmond, C.S.B., Souch, C., Hubble, M.D., 1996. Influence of tree cover on summertime surface energy balance fluxes, San Gabriel Valley, Los Angeles. Clim. Res. 6 (1), 45–57. https://doi.org/10.3354/cr006045.

Huang, J., Jones, P., Zhang, A., Peng, R., Li, X., Wai Chan, P., 2020. Urban building energy and climate (UrBEC) simulation: example application and field evaluation in Sai Ying Pun, Hong Kong. Energy Build. 207 https://doi.org/10.1016/j.enbuild.2019.109580.

Institute Cartographic and Geological of Catalonia (ICGC), 2019. LiDAR Data. https://www.icgc.cat/es/Descargas/Elevaciones/Datos-lidar (accessed 16 July 2019).

ISO, 1998. ISO 7726 Ergonomics of the Thermal Environment — Instruments for Measuring Physical Quantities, 1998. ISO Standard, pp. 1–56.

Janhäll, S., 2015, March 1. Review on urban vegetation and particle air pollution - Deposition and dispersion. Atmos. Environ. https://doi.org/10.1016/j.atmosenv.2015.01.052 (Elsevier Ltd).
Jendritzky, G., de Dear, R., Havenith, G., 2012. UTCI-why another thermal index? Int. J. Biometeorol. 56 (3), 421–428. https://doi.org/10.1007/s00484-011-0513-7.
Jin, S., Guo, J., Wheeler, S., Kan, L., Che, S., 2014. Evaluation of impacts of trees on PM2.5 dispersion in urban streets. Atmos. Environ. 99, 277–287. https://doi.org/10.1016/j.atmosenv.2014.10.002.
Johansson, E., Emmanuel, R., 2006. The influence of urban design on outdoor thermal comfort in the hot, humid city of Colombo, Sri Lanka. Int. J. Biometeorol. 51 (2), 119–133. https://doi.org/10.1007/s00484-006-0047-6.
Krayenhoff, E.S., Christen, A., Martilli, A., Oke, T.R., 2014. A multi-layer radiation model for urban Neighbourhoods with trees. Bound.-Layer Meteorol. 151 (1), 139–178. https://doi.org/10.1007/s10546-013-9883-1.
Krayenhoff, E.S., Santiago, J.L., Martilli, A., Christen, A., Oke, T.R., 2015. Parametrization of drag and turbulence for urban Neighbourhoods with trees. Bound.-Layer Meteorol. 156 (2), 157–189. https://doi.org/10.1007/s10546-015-0028-6.
Krayenhoff, E.S., Jiang, T., Christen, A., Martilli, A., Oke, T.R., Bailey, B.N., Nazarian, N., Voogt, J., Giometto, M., Stastny, A., Crawford, B.R., 2020. A multi-layer urban canopy meteorological model with trees (BEP-tree): street tree impacts on pedestrian-level climate. Urban Clim. 32 https://doi.org/10.1016/j.uclim.2020.100590.
Krayenhoff, E.S., Broadbent, A.M., Zhao, L., Georgescu, M., Middel, A., Voogt, J.A., Martilli, A., Sailor, D., Erell, E., 2021. Cooling hot cities: systematic and critical review of the numerical modelling literature. Environ. Res. Lett. 16 (5), 053007.
Lachapelle, J.A., Krayenhoff, E.S., Middel, A., Meltzer, S., Broadbent, A.M., Georgescu, M., 2022. A microscale three-dimensional model of urban outdoor thermal exposure (TUF-pedestrian). Int. J. Biometeorol. 1–16.
Lalic, B., Mihailovic, D.T., 2004. An empirical relation describing leaf-area density inside the forest for environmental modeling. J. Appl. Meteorol. 43 (4), 641–645. https://doi.org/10.1175/1520-0450(2004)043<0641:AERDLD>2.0.CO;2.
Lee, S.H., 2011. Further development of the vegetated urban canopy model including a grass-covered surface parametrization and photosynthesis effects. Bound.-Layer Meteorol. 140 (2), 315–342. https://doi.org/10.1007/s10546-011-9603-7.
Lee, S.H., Park, S.U., 2008. A vegetated urban canopy model for meteorological and environmental modelling. Bound.-Layer Meteorol. 126 (1), 73–102. https://doi.org/10.1007/s10546-007-9221-6.
Lemonsu, A., Grimmond, C.S.B., Masson, V., 2004. Modeling the surface energy balance of the core of an old Mediterranean City: Marseille. J. Appl. Meteorol. 43 (2), 312–327. https://doi.org/10.1175/1520-0450(2004)043<0312:MTSEBO>2.0.CO;2.
Lin, B. S., & Lin, Y. J. (2010). Cooling effect of shade trees with different characteristics in a subtropical urban park. HortScience, 45(1), 83–86. Doi:10.21273/hortsci.45.1.83.
Martilli, A., Clappier, A., Rotach, M.W., 2002. An urban surface exchange parameterisation for mesoscale models. Bound.-Layer Meteorol. 104 (2), 261–304. https://doi.org/10.1023/A:1016099921195.
Matzarakis, A., Rutz, F., Mayer, H., 2010. Modelling radiation fluxes in simple and complex environments: basics of the RayMan model. Int. J. Biometeorol. 54 (2), 131–139. https://doi.org/10.1007/s00484-009-0261-0.
Mayer, H., Höppe, P., 1987. Thermal comfort of man in different urban environments. Theor. Appl. Climatol. 38 (1), 43–49. https://doi.org/10.1007/BF00866252.
Meili, N., Manoli, G., Burlando, P., Bou-Zeid, E., Chow, W.T.L., Coutts, A.M., Daly, E., Nice, K.A., Roth, M., Tapper, N.J., Velasco, E., Vivoni, E.R., Fatichi, S., 2020. An urban ecohydrological model to quantify the effect of vegetation on urban climate and hydrology (UT&C v1.0). Geosci. Model Dev. 13 (1), 335–362. https://doi.org/10.5194/gmd-13-335-2020.
Middel, A., Krayenhoff, E.S., 2019. Micrometeorological determinants of pedestrian thermal exposure during record-breaking heat in Tempe, Arizona: introducing the MaRTy observational platform. Sci. Total Environ. 687, 137–151. https://doi.org/10.1016/j.scitotenv.2019.06.085.
Mussetti, G., Brunner, D., Henne, S., Allegrini, J., Krayenhoff, E.S., Schubert, S., Feigenwinter, C., Vogt, R., Wicki, A., Carmeliet, J., 2020. COSMO-BEP-tree v1.0: a coupled urban climate model with explicit representation of street trees. Geosci. Model Dev. 13 (3), 1685–1710. https://doi.org/10.5194/gmd-13-1685-2020.
Nazarian, N., Scott Krayenhoff, E., Martilli, A., 2020. A one-dimensional model of turbulent flow through "urban" canopies (MLUCM v2.0): updates based on large-eddy simulation. Geosci. Model Dev. 13 (3), 937–953. https://doi.org/10.5194/gmd-13-937-2020.
Nowak, D.J., 1996. Estimating leaf area and leaf biomass of open-grown deciduous urban trees. For. Sci. 42 (4), 504–507. https://doi.org/10.1093/forestscience/42.4.504.
Oke, T.R., 1982. The energetic basis of the urban heat island. Q. J. R. Meteorol. Soc. 108 (455), 1–24. https://doi.org/10.1002/qj.49710845502.
Oke, T.R., 1989. The micrometeorology of the urban forest. Philos. Trans. R. Soc. Lond. B 324 (1223), 335–349. https://doi.org/10.1098/rstb.1989.0051.
Oke, T.R., Mills, G., Christen, A., Voogt, J.A., 2017. Urban climates. Cambridge University Press, pp. 1–525. https://doi.org/10.1017/9781139016476.
Oliveira, S., Andrade, H., Vaz, T., 2011. The cooling effect of green spaces as a contribution to the mitigation of urban heat: a case study in Lisbon. Build. Environ. 46 (11), 2186–2194. https://doi.org/10.1016/j.buildenv.2011.04.034.
Papangelis, G., Tombrou, M., Dandou, A., Kontos, T., 2012. An urban "green planning" approach utilizing the weather research and forecasting (WRF) modeling system. A case study of Athens, Greece. Landsc. Urban Plan. 105 (1–2), 174–183. https://doi.org/10.1016/j.landurbplan.2011.12.014.
Pauleit, S., Jones, N., Garcia-Martin, G., Garcia-Valdecantos, J.L., Rivière, L.M., Vidal-Beaudet, L., Bodson, M., Randrup, T.B., 2002. Tree establishment practice in towns and cities - results from a European survey. Urban Forest. Urban Green. 1 (2), 83–96. https://doi.org/10.1078/1618-8667-00009.
Revi, A., Satterthwaite, D.E., Aragón-Durand, F., Corfee-Morlot, J., Kiunsi, R.B.R., Pelling, M., Roberts, D.C., Solecki, W., 2014. Urban areas. In: Field, C.B., Barros, V. R., Dokken, D.J., Mach, K.J., Mastrandrea, M.D., Bilir, T.E., Chatterjee, M., Ebi, K.L., Estrada, Y.O., Genova, R.C., Girma, B., Kissel, E.S., Levy, A.N., MacCracken, S., Mastrandrea, P.R., White, L.L. (Eds.), Climate Change 2014: Impacts, Adaptation, and Vulnerability. Part A: Global and Sectoral Aspects. Contribution of Working Group II to the Fifth Assessment Report of the Intergovernmental Panel on Climate Change. Cambridge University Press, Cambridge, United Kingdom and New York, NY, USA, pp. 535–612.
Ribeiro, I., Martilli, A., Falls, M., Zonato, A., Villalba, G., 2021. Highly resolved WRF-BEP/BEM simulations over Barcelona urban area with LCZ. Atmos. Res. 248. https://doi.org/10.1016/j.atmosres.2020.105220.
Ryu, Y.H., Bou-Zeid, E., Wang, Z.H., Smith, J.A., 2016. Realistic representation of trees in an urban canopy model. Bound.-Layer Meteorol. 159 (2), 193–220. https://doi.org/10.1007/s10546-015-0120-y.
Salamanca, F., Martilli, A., 2010. A new building energy model coupled with an urban canopy parameterization for urban climate simulations-part II. Validation with one dimension off-line simulations. Theor. Appl. Climatol. 99 (3–4), 345–356. https://doi.org/10.1007/s00704-009-0143-8.
Salmond, J.A., Tadaki, M., Vardoulakis, S., Arbuthnott, K., Coutts, A., Demuzere, M., Wheeler, B.W., 2016. Health and Climate Related Ecosystem Services Provided by Street Trees in the Urban Environment. Environmental Health: A Global Access Science Source. BioMed Central Ltd. https://doi.org/10.1186/s12940-016-0103-6
Santiago, J.L., Martilli, A., 2010. A dynamic urban canopy parameterization for mesoscale models based on computational fluid dynamics Reynolds-averaged Navier-stokes microscale simulations. Bound.-Layer Meteorol. 137 (3), 417–439. https://doi.org/10.1007/s10546-010-9538-4.
Segura, R., Badia, A., Ventura, S., Gilabert, J., Martilli, A., Villalba, G., 2021. Sensitivity study of PBL schemes and soil initialization using the WRF-BEP-BEM model over a Mediterranean coastal city. Urban Clim. 39 https://doi.org/10.1016/j.uclim.2021.100982.
Shashua-Bar, L., Hoffman, M.E., 2000. Vegetation as a climatic component in the design of an urban street. An empirical model for predicting the cooling effect of urban green areas with trees. Energy Build. 31 (3), 221–235. https://doi.org/10.1016/S0378-7788(99)00018-3.
Shashua-Bar, L., Pearlmutter, D., Erell, E., 2011. The influence of trees and grass on outdoor thermal comfort in a hot-arid environment. Int. J. Climatol. 31 (10), 1498–1506. https://doi.org/10.1002/joc.2177.
Shiflett, S.A., Liang, L.L., Crum, S.M., Feyisa, G.L., Wang, J., Jenerette, G.D., 2017. Variation in the urban vegetation, surface temperature, air temperature nexus. Sci. Total Environ. 579, 495–505. https://doi.org/10.1016/j.scitotenv.2016.11.069.
Taha, H., Akbari, H., Rosenfeld, A., 1991. Heat island and oasis effects of vegetative canopies: Micro-meteorological field-measurements. Theor. Appl. Climatol. 44 (2), 123–138. https://doi.org/10.1007/BF00867999.

Thorsson, S., Lindberg, F., Eliasson, I., Holmer, B., 2007. Different methods for estimating the mean radiant temperature in an outdoor urban setting. Int. J. Climatol. 27, 1983–1993. https://doi.org/10.1002/joc.1537.

Vico, G., Revelli, R., Porporato, A., 2014. Ecohydrology of street trees: design and irrigation requirements for sustainable water use. Ecohydrology 7 (2), 508–523. https://doi.org/10.1002/eco.1369.

Wieringa, J., 1986. Roughness-dependent geographical interpolation of surface wind speed averages. Q. J. R. Meteorol. Soc. 112 (473), 867–889. https://doi.org/10.1002/qj.49711247316.

Zhang, Z., Lv, Y., Pan, H., 2013. Cooling and humidifying effect of plant communities in subtropical urban parks. Urban Forest. Urban Green. 12 (3), 323–329. https://doi.org/10.1016/j.ufug.2013.03.010.